

**CONFIDENTIAL**

Copy 5  
RM L56E16



**NACA**

# RESEARCH MEMORANDUM

BLOWING OVER THE FLAPS AND WING LEADING EDGE OF A THIN  
49° SWEPT WING-BODY-TAIL CONFIGURATION IN COMBINATION  
WITH LEADING-EDGE DEVICES

By H. Clyde McLemore and Marvin P. Fink

Langley Aeronautical Laboratory  
Langley Field, Va.

CLASSIFICATION CHANGED

UNCLASSIFIED

*NACA RM 56-137*  
*affiliated*  
*Dec 16, 1958*  
*1077 7-2-58*

CLASSIFIED DOCUMENT

This material contains information affecting the National Defense of the United States within the meaning of the espionage laws, Title 18, U.S.C., Secs. 793 and 794, the transmission or revelation of which in any manner to an unauthorized person is prohibited by law.

**NATIONAL ADVISORY COMMITTEE  
FOR AERONAUTICS**

**WASHINGTON**

July 20, 1956

**CONFIDENTIAL**

## NATIONAL ADVISORY COMMITTEE FOR AERONAUTICS

## RESEARCH MEMORANDUM

BLOWING OVER THE FLAPS AND WING LEADING EDGE OF A THIN  
49° SWEEP WING-BODY-TAIL CONFIGURATION IN COMBINATION  
WITH LEADING-EDGE DEVICES

By H. Clyde McLemore and Marvin P. Fink

SUMMARY

An investigation has been conducted in the Langley full-scale tunnel to determine the effects on the low-speed aerodynamic characteristics of blowing air over the trailing-edge flap of a large-scale wing-body-tail model. The wing and horizontal tail have an aspect ratio of 3.5, taper ratio of 0.3, leading-edge sweep of 49°, and NACA 65A006 airfoil sections parallel to the plane of symmetry. The trailing-edge air was ejected over highly deflected half- and full-span flaps in combination with several leading-edge-flow control devices including blowing from a slot in the wing leading edge. The momentum coefficient range investigated was 0 to 0.16 for the trailing-edge blowing and 0 to 0.025 for the leading-edge blowing. Most of the tests were conducted at a Reynolds number of  $5.2 \times 10^6$  corresponding to a Mach number of 0.08.

Blowing over highly deflected trailing-edge flaps produced lift increments approximately equal to values predicted by potential theory for moderate values of momentum coefficient. Effective full-span leading-edge-stall control devices must be used when blowing is applied over flaps if appreciable lift gains are to be realized in the high angle-of-attack range. Blowing over inboard half-span flaps or blowing applied outboard at the wing leading edge provides marked improvement in the effectiveness of outboard located ailerons.

INTRODUCTION

The problem of obtaining acceptable landing speeds for high-speed airplanes has become increasingly severe in the past few years due to increased wing loadings and reduced effectiveness of conventional high-lift devices when applied to highly swept wings. The necessity of obtaining increased lift for these airplanes at a given attitude has

~~CONFIDENTIAL~~

prompted research into methods of obtaining higher lift through increased flap effectiveness and improved leading-edge-stall control. One of the more recent considerations for achieving an improvement in landing and take-off performance is boundary-layer control by blowing a high energy stream of air over surfaces otherwise subject to air-flow separation.

This system of boundary-layer control is by no means new in principle. The investigations reported in references 1, 2, and 3 (to mention only a few) had indicated that considerable improvement in the lift characteristics of airfoils could be realized. Until recent years, however, the necessary equipment (motors, pumps, and plumbing) for providing boundary-layer control was so heavy, inefficient, and bulky that the net gain in lift of a complete airplane configuration equipped for boundary-layer control by blowing was determined to be negligible. The use of the jet engine, however, provides a convenient and available air pumping source for a blowing-type boundary-layer control system, utilizing bleed air either from a compressor stage or from the engine tailpipe, without any appreciable weight penalty. Boundary-layer control, therefore, has become the subject of renewed interest as a possible means of either increasing the load-carrying capabilities of present-day aircraft or providing decreased landing and take-off speeds.

The present paper presents the results of tests with and without boundary-layer control by blowing over highly deflected half- and full-span flaps and over the wing leading edge of a modern fighter-type-airplane model. The primary purpose of this investigation was to determine the lift gains to be attained by the blowing-type boundary-layer control and the amount of air required to produce these gains. Results are also given to show the effects of blowing on the trim requirements and horizontal-tail effectiveness and on the wing leading-edge-flow control devices required to prevent leading-edge separation.

The model used in the present investigation was a large-scale, wing-body-tail configuration having NACA 65A006 airfoil sections parallel to the plane of symmetry, an aspect ratio of 3.5, taper ratio of 0.3, and  $49^\circ$  of sweep at the leading edge.

The tests of this investigation were conducted in the Langley full-scale tunnel for a range of angles of attack, flap angles, aileron angles, and tail incidence angles with most of the tests conducted at a Reynolds number of  $5.2 \times 10^6$  corresponding to a Mach number of 0.08.

~~CONFIDENTIAL~~

COEFFICIENTS AND SYMBOLS

$C_L$	lift coefficient, $\frac{\text{Lift}}{q_o S}$
$\Delta C_{L_{\alpha=0^\circ}}$	increment in lift coefficient due to flap deflection at $\alpha = 0^\circ$
$C_{L_{\max}}$	maximum lift coefficient
$C_D$	drag coefficient, $\frac{\text{Drag}}{q_o S}$ (drag equivalent of pumping power not included)
$C_m$	pitching-moment coefficient about $\bar{c}/4$ (see fig. 1), $\frac{\text{Pitching moment}}{q_o S \bar{c}}$
$dC_m/dC_L$	rate of change of pitching-moment coefficient with lift coefficient
$C_l$	rolling-moment coefficient, $\frac{\text{Rolling moment}}{q_o S b}$
$C_n$	yawing-moment coefficient, $\frac{\text{Yawing moment}}{q_o S b}$
$C_Q$	flow coefficient, $Q/V_o S$
$C_\mu$	momentum coefficient, $\frac{Q_p j V_j}{q_o S}$ or $\frac{G V_j}{g q_o S}$
$q_o$	free-stream dynamic pressure, $\frac{1}{2} \rho_o V_o^2$
$L/D$	lift-drag ratio
$c$	local wing chord measured parallel to plane of symmetry, ft
$\bar{c}$	mean aerodynamic chord, $\frac{2}{S} \int_0^{b/2} c^2 dy$ , ft

~~CONFIDENTIAL~~

$c_{av}$	average chord of wing measured parallel to plane of symmetry $S/b$ , ft
$b$	wing span, ft
$y$	spanwise distance measured perpendicular to plane of symmetry, ft
$S$	area of wing, sq ft
$R$	Reynolds number based on mean aerodynamic chord
$V_o$	free-stream velocity, ft/sec
$V_j$	velocity of ejected air at slot, ft/sec
$\rho_o$	mass density of free-stream air, slugs/cu ft
$\rho_j$	mass density of ejected air at slot, slugs/cu ft
$Q$	volume flow of air blown out of slot, cu ft/sec
$G$	weight flow of air from slot, lb/sec
$g$	acceleration due to gravity, ft/sec <sup>2</sup>
$\alpha$	angle of attack, deg
$\epsilon$	effective downwash, deg
$\delta_f$	flap deflection (relative to wing-chord plane) measured perpendicular to flap hinge line, deg
$\delta_a$	aileron deflection (relative to wing-chord plane) measured perpendicular to aileron hinge line (positive when right aileron trailing edge down), deg
$i_t$	horizontal-tail deflection (relative to wing-chord plane) measured parallel to plane of symmetry (positive when trailing edge down), deg

## Subscripts:

LE	wing leading edge
TE	wing trailing edge
R	right wing

MODEL

The model used for this investigation was a large-scale research model having the geometric characteristics shown in figure 1. The wing has a leading-edge sweep of  $49^{\circ}$ , an aspect ratio of 3.5, a taper ratio of 0.3, and NACA 65A006 airfoil sections parallel to the plane of symmetry. A photograph of the model mounted for tests in the Langley full-scale tunnel is given as figure 2. The model was equipped with 0.24c flaps and ailerons, measured from the hinge line, with the ailerons being capable of deflection as outboard flaps.

The leading-edge-flow control devices used in this investigation were a 0.15c slat, a 0.013c increase in the leading-edge radius similar in profile to the WADC inflatable boot, and an outboard wing leading-edge blowing jet. The slat and radius increase were segmented so that portions could be tested alone or in combination with the other devices. The slat used was not an integral part of the wing but was mounted onto the unmodified wing leading edge with lower surface brackets aligned with the plane of symmetry of the model. The radius increase, when used in combination with the 0.60b/2 slat, extended from the inboard end of the slat to the fuselage. When the leading-edge-radius increase was used in combination with leading-edge blowing, the radius increase extended over the entire span. Sectional views of these high-lift and flow control devices are presented in figure 3.

Just ahead of the flaps and ailerons a slot opened into the wing trailing edge (see fig. 3) through which the trailing-edge boundary-layer control air was ejected. The slot was constructed so that the slot gap could be varied to control the amount and rate of flow of air ejected over half- or full-span flaps.

To make possible some exploratory tests of leading-edge blowing, a slot was constructed as near to the wing leading edge as practical (0.005c<sub>av</sub>) and extended over the outboard 38 percent of the right wing only. The available high-pressure air supply for the leading-edge-blowing tests was limited and this dictated the extent of wing span investigated.

The model had an all-movable horizontal tail mounted on the fuselage center line at a tail length of approximately 1.5c.

## APPARATUS

### AIR SUPPLY

The air supply for the trailing-edge-blowing tests was obtained from a modified J-34 compressor mounted in the fuselage which was driven by two 200-horsepower electric motors. The air to the compressor was supplied through a fuselage nose inlet. The compressor exhausted into a plenum chamber which supplied the air to the flaps and ailerons through internal wing ducts. The compressor, as used, was capable of producing a maximum pressure of 1.4 atmospheres at the exit slot and a maximum weight flow rate of approximately 29 pounds per second.

The air supply for the leading-edge-blowing tests was supplied from an external source and was brought on board the model through an external duct attached to the lower surface of the right wing. The pressure available for the leading-edge-blowing tests was approximately 1.9 atmospheres with a maximum weight flow rate of 1.7 pounds per second.

### INSTRUMENTATION

Shielded thermocouples and rakes of total and static pressure tubes were mounted in the wing ducts upstream of the blowing slots and were used to determine the flow quantity for the flap and aileron blowing tests. Shielded thermocouples were also used in the leading-edge-blowing duct to determine the duct air temperature, but the weight flow was determined from orifice pressure and temperature measurements in the supply tube.

The normal force of the horizontal tail, which was used to determine the effective downwash at the tail, was determined by the use of a strain gage attached to the left horizontal-tail pivot shaft.

### TESTS

The static longitudinal and lateral control characteristics of the model were determined from force measurements obtained from the tunnel scale balance system for a range of angles of attack from approximately  $-4^{\circ}$  to  $23^{\circ}$ . An index of the test conditions for the various configurations used in this investigation is given in the following table:

~~CONFIDENTIAL~~

Wing leading-edge configuration	$\delta_f$ , deg	$\delta_a$ , deg		$i_t$ , deg	Momentum coefficient range		
					Trailing edge		Leading edge
		Left	Right		Half-span	Full-span	$0.38b/2$
Basic	0	0	0	0	0	0	0
	40	0	0	0	0 to 0.064	0	0
	50	0	0	0	0 to 0.064	0	0
	60	0	0	0	0 to 0.064	0	0
0.40b/2 slat	60	0	0	0	0.027 to 0.099	0	0
0.60b/2 slat	60	0	0	0	0 to 0.099	0	0
0.85b/2 slat	60	0	0	0	0 to 0.099	0	0
0.60b/2 slat plus inboard radius increase	40	0	0	0	0 to 0.099	0	0
	50	0	0	0	0 to 0.099	0	0
	60	0	0	10 to -25	0 to 0.099	0	0
	40	40	40	0	-----	0 to 0.099	0
	50	50	50	0	-----	0 to 0.099	0
	60	60	60	10 to -25	-----	0 to 0.099	0
	60	0	-10 to 30	0	0 to 0.099	0	0
	60	30	20 to 60	0 to -25	-----	0 to 0.099	0
Full-span radius increase	60	0	-10 to 30	0	0 to 0.164	0	0 to 0.025

The hemispherical nose inlet fairing (fig. 1) was installed for all the tests for which trailing-edge blowing was not applied.

Preliminary tests showed that woolen tufts attached to the upper surface of the wing had negligible effects on the force and moment characteristics of the model and, therefore, were left on the wing for flow-visualization studies throughout the investigation.

The basic leading-edge configuration with flaps and ailerons neutral was tested at Reynolds numbers of  $3.02 \times 10^6$ ,  $5.20 \times 10^6$ , and  $6.20 \times 10^6$ ; however, all of the remaining tests were conducted at a Reynolds number of  $5.20 \times 10^6$  corresponding to a Mach number of 0.08.

#### CORRECTIONS

The data have been corrected for airstream misalignment, buoyancy, and jet boundary effects. For the trailing-edge-blowing tests a correction to the drag characteristics resulting from taking the air on board the model was unnecessary inasmuch as the air delivered to the compressor was obtained from the airstream through a fuselage nose inlet.



For the leading-edge-blowing tests, however, the air entered the model from an external source, and calculations were made to determine the drag equivalent to taking air on board the model. For the flow rates used in this investigation the drag equivalent (0.002 maximum) was considered to be unimportant for the purpose of this investigation and, therefore, was not applied.

The drag equivalent of the pumping power required for the trailing- and leading-edge blowing has not been included in the drag data. The leading-edge blowing air was brought onto the scale balance system through a flexible connector aligned in the direction of the side force at some distance below the model. The pressure reaction of the blowing air, therefore, was in the direction of this force thus eliminating the need for tare corrections to the lift, drag, and pitching moment. The tare corrections to the rolling- and yawing-moment data were a function of the duct pressure reaction forces and the geometric distances of the tunnel setup. Static calibrations were made to check the alignment of the duct setup which confirmed the lack of tares for the lift, drag, and pitching moments and the ability to calculate the rolling- and yawing-moment tares as a function of the duct pressure.

Inasmuch as the leading-edge blowing was applied only over the right wing, the total effect of leading-edge blowing presented in this report was determined by doubling the increments of lift, pitching moment, and drag obtained when blowing was applied over the right wing. Subsequent tests conducted with the present model with leading-edge blowing applied over the outboard portions of both wings have shown that doubling the lift increments is a valid procedure. The validity of this procedure for determining the drag and pitching-moment data, however, has not been definitely established.

### PRESENTATION OF RESULTS

The figures presenting the results of the present investigation are grouped as follows:

	<u>Figure</u>
Basic wing characteristics for several Reynolds numbers . . .	4
Effect of trailing-edge blowing over half-span flaps for the basic wing configuration . . . . .	5
Summary of the effect of half-span trailing-edge blowing on half-span flap effectiveness at $\alpha = 0^\circ$ . . . . .	6
Effect of several partial- and full-span leading-edge-flow control devices . . . . .	7 to 15
Effect of full-span trailing-edge blowing over several combinations of full-span deflected flaps . . . . .	16 and 18

Figure

Summary of the effect of full-span trailing-edge blowing on full-span flap effectiveness at $\alpha = 0^\circ$ . . . . .	17
Effect of half-span trailing-edge blowing on the longitudinal control and trim characteristics . . . . .	19
Effect of full-span trailing-edge blowing on the longitudinal control and trim characteristics . . . . .	20
Effect of half- and full-span trailing-edge blowing on the effective downwash characteristics . . . . .	21
Effect of half- and full-span trailing-edge blowing on the lift-drag ratio . . . . .	22 and 23
Effect of half- and full-span trailing-edge blowing, and leading-edge blowing on the aileron characteristics . .	24 and 25

RESULTS AND DISCUSSION

With the available blower air supply, it was possible to cover a range of trailing-edge blowing momentum coefficients up to approximately 0.16. This range represents either a compressor bleed system in the low  $C_\mu$  range ( $C_\mu < 0.05$ ) or a tailpipe exhaust bleed system at the greater  $C_\mu$  values. Preliminary tests made with velocity ratio  $V_j/V_0$  and flow coefficient  $C_Q$  varied independently by varying slot height for a range of  $V_j/V_0$  and  $C_Q$  from 2.5 to 8 and 0.0016 to 0.0105, respectively, showed that momentum coefficient  $C_\mu$  for a properly aligned jet was the primary factor affecting the lift gains to be attained by blowing air over trailing-edge flaps. (This finding has also been established independently and reported by other investigators.) With this fact established, the data of the present report are presented using  $C_\mu$  as the correlating factor.

In order to determine whether any significant Reynolds number effects existed, tests were made over a Reynolds number range from  $3.02 \times 10^6$  to  $6.20 \times 10^6$  for the basic configuration with flaps and ailerons neutral. The results of the tests (fig. 4) did not show any appreciable Reynolds number effects. Preliminary tests for various rates of trailing-edge blowing also did not show any significant Reynolds number effects. All subsequent tests, consequently, were made for a Reynolds number of  $5.20 \times 10^6$ .

## LIFT CHARACTERISTICS

## Half-Span Flaps

Effect of trailing-edge blowing and flap deflection at  $\alpha = 0^\circ$ .- The basic effectiveness of the blowing jet on the flapped wing at  $\alpha = 0^\circ$  is indicated by the results presented in figure 6(a) showing the increment of  $C_L$  for a given amount of blowing momentum  $C_\mu$  for flap angles of  $40^\circ$ ,  $50^\circ$ , and  $60^\circ$ . It is evident that only a small amount of jet energy is required essentially to eliminate separated flow over the deflected flap (the portion of the curve for which the rate of increase of  $\Delta C_L$  with  $C_\mu$  markedly decreases - often referred to as the "knee" of the  $\Delta C_L - C_\mu$  curve). The knee of the curve correlated well with the flow cleanup noted by the observation of wool tufts attached to the upper surface of the flaps. It is evident from these results that, for a given amount of momentum, the greatest gain in lift to be obtained from this type of boundary-layer control system is accomplished by eliminating the separated flow over the flap. If additional momentum is available from the pumping source, then further gains in lift are available but at a much lesser rate. For example, with the flap deflected  $60^\circ$  a blowing  $C_\mu$  of 0.015 produces an increment of  $C_L$  of about 0.35, whereas only an additional  $\Delta C_L$  of about 0.07 is obtained for an increase in  $C_\mu$  to a value of 0.06. It may be noted that for this same range of  $C_\mu$  the rate of flow of the downward component of jet momentum is about one-half of the additional lift increment obtained. The fourfold increase in  $C_\mu$  for an additional one-fifth gain in  $\Delta C_L$  over and above that required for eliminating separation may not be practical for most compressor bleed systems. For a tailpipe bleed or a large mass flow arrangement, however, where pumping power expended is not a major consideration all available lift gains could be utilized, provided the configuration can be trimmed.

The increase of  $\Delta C_L$  with flap deflection for a given value of  $C_\mu$  in excess of that required for cleanup is reduced somewhat for the  $60^\circ$  flapped configuration (fig. 6(a)). This reduction of lift effectiveness is at least in part the result of increased losses at the ends of the flaps with the increased deflection angles. The inboard and outboard ends of the flaps, when deflected to large angles, were definitely experiencing flow breakdown even with blowing applied as noted in the tuft diagrams of figure 8.

The experimental lift results obtained at  $\alpha = 0^\circ$  are summarized as a function of flap angle in figure 6(b). The results of theoretical calculations of the potential lift increment due to deflecting flaps as determined by the method of reference 4 are also included in this figure. A comparison of figures 6(a) and 6(b) shows that for the flap

angles investigated the calculated potential lift values are in reasonable agreement with those obtained experimentally at the knee of the  $\Delta C_L - C_{\mu}$  curve.

Effect of trailing-edge blowing, flap deflection, and leading-edge devices at angles of attack.- Of major consideration for any flapped wing, once the flap effectiveness has been established at zero or low angles of attack, is the ability to maintain the flapped lift gains to the stall. It has been the experience of many thin swept-wing configurations that the angle of attack for maximum lift has been severely limited by leading-edge separation. For the configuration investigated, this is clearly demonstrated by the results given in figure 5 which shows that the flapped wing with blowing but without a leading-edge device experiences practically no increase in  $CL_{max}$  over the basic unflapped wing - even at high values of  $C_{\mu}$ .

In order to gain more insight as to the nature of the flow field over the wing before embarking on a comprehensive leading-edge flow-control program, a study was made of the wing stall pattern with and without blowing applied (fig. 8). The results of these flow studies indicated that an outboard leading-edge device would be required to alleviate the tip stall. Tests were therefore conducted with leading-edge slats having spans of  $0.40b/2$ ,  $0.50b/2$ , and  $0.60b/2$ , without blowing over  $40^\circ$  deflected flaps, to determine the extent of leading-edge-slat span required to give acceptable lift and pitching-moment characteristics and to serve as a basis for comparing the overall effects of boundary-layer control. The  $0.40b/2$  and  $0.50b/2$  slats (data not presented) provided stability at  $CL_{max}$  but did not maintain the flap lift increment to  $CL_{max}$ . A slat span of approximately  $0.60b/2$  was found to be sufficient to maintain the flap lift increment to  $CL_{max}$  and give only a slight instability at  $CL_{max}$ , so several tests were conducted with the  $0.60b/2$  slat installed in combination with flaps deflected  $60^\circ$ . The results of these tests are shown in figure 7. Without blowing, the lift curve was made essentially straight to  $CL_{max}$ ; however, with blowing applied the lift-curve slope began to decrease rather rapidly before  $CL_{max}$  was reached. This was not expected originally, since the outboard wing sections which had stalled first without slats installed were believed to be adequately influenced by the slat selected. It was observed, however, from tuft studies (fig. 8) that a marked region of flow disturbance over the inboard portion of the wing resulted from leading-edge separation inboard of the slat. It was apparent, therefore, that with trailing-edge blowing applied some full-span leading-edge-flow control device would be required to prevent the inboard leading-edge separation and alleviate the reduction in lift-curve slope.

The first such device studied was a 0.013c leading-edge radius increase installed inboard of the 0.60b/2 slat which, as far as flow control is concerned, could be considered similar to at least one present-day fighter configuration which has outboard leading-edge chord-extension and inboard leading-edge droop. A comparison of the results obtained for this configuration with those obtained for the slat alone (fig. 9) shows that the lift-curve-slope reduction at high lift was essentially eliminated. For the largest  $C_{\mu}$  investigated ( $C_{\mu} = 0.099$ ), which would produce the greatest induced local upwash angles and therefore the most severe leading-edge separation, the addition of the radius increased  $C_{L_{max}}$  from 1.47 to 1.67. Tuft diagrams of these configurations (fig. 10) show the inboard flow disturbance to be considerably reduced with the radius increase installed.

In order to show more graphically the effect of increasing the span of leading-edge-flow control devices, tests were conducted for slat spans varying from 0.40b/2 to the fuselage juncture (full-span or 0.85b/2) for several values of  $C_{\mu}$ . Increasing the slat span progressively alleviated the reduced lift-curve slope (fig. 11) resulting in an increase in  $C_L$  ( $C_{\mu} = 0.099$ ) from 1.30 for the 0.40b/2 slat to a value of 1.67 for the full-span slat configuration.

The slat configuration employed for this investigation had a stream-wise slat angle of  $25^{\circ}$  which was the largest angle that could be used without precipitating separation of the flow at the trailing edge of the slat. It is believed that, if a slat configuration with improved slot geometric characteristics could have been used, larger deflection angles would have been possible and the angle of attack for  $C_{L_{max}}$  would have been increased resulting in some further increases in  $C_{L_{max}}$ .

Another leading-edge-flow control device used in this investigation was a full-span (0.013c) leading-edge-radius increase. The maximum lift of this configuration (fig. 12) was not as large as that obtained for the slat-plus-radius or full-span slat configurations (figs. 9 and 11, respectively), because the full-span-radius increase was unable to control the leading-edge separation (especially in the region of the wing tips, see fig. 14) to as high an angle of attack as did the other full-span leading-edge devices. Additional outboard treatment would therefore be required.

Effect of leading-edge blowing at high angles of attack.- In an attempt to control further the leading-edge separation associated with the full-span radius-increase configuration, tests were made with leading-edge blowing applied over the outboard 0.38b/2 of the right wing in combination with the full-span radius-increase.

Leading-edge blowing at a velocity of the order of 1,000 ft/sec ( $C_{\mu LE} = 0.025$ ) greatly improved the maximum lift values as compared with those obtained for the full-span radius-alone configuration (fig. 13) by considerably extending the angle of attack for maximum lift. For a value of  $C_{\mu TE}$  equal to 0.164,  $C_{L_{max}}$  was increased from a value of 1.5 at  $\alpha = 11.4^\circ$  to a value of 1.78 at a value of  $\alpha = 16.5^\circ$ .

Tuft diagrams are presented as figure 14 to illustrate the difference in the type of flow existing over the full-span radius-increase configuration when leading-edge blowing is applied. The significant difference in the flow over the wing is that, with leading-edge blowing applied, attached flow is maintained over the outboard wing sections to considerably higher angles of attack.

For comparable trailing-edge-blowing rates the leading-edge blowing in combination with the full-span-radius increase produced  $C_{L_{max}}$  values of the same order of magnitude as those obtained for the slat-plus-radius or full-span slat configurations. While model construction did not allow different extents of leading-edge treatment to reach an optimum leading-edge-blowing application, the results of the limited tests did show encouraging possibilities of leading-edge blowing when used in combination with the full-span-radius increase.

Effect of trailing-edge blowing and flap deflection for one of the better leading-edge configurations. - In order to provide more complete information over a wider range of flap deflections than that normally considered in practice, the effects of flap deflection and momentum coefficient for one of the better leading-edge configurations were tested in combination with the 0.60b/2 slat plus radius increase for several values of  $C_{\mu}$  (fig. 15). The characteristic flap effectiveness at low angles of attack and the behavior of the wing at high angles of attack discussed previously are shown to be consistent for the range of flap angles investigated.

In summation, the lift characteristics presented in figures 5 to 15 show that trailing-edge blowing over deflected flaps, for even very low momentum coefficients, will produce values of lift equal to the potential flow lift values. The data also show that the problems of wing leading-edge separation are more severe with the application of trailing-edge blowing. To realize any appreciable gain in the maximum lift with trailing-edge blowing applied, full-span leading-edge-flow control devices must be used to maintain linear lift curves through the usable angle-of-attack range. It should be noted, however, that although the particular leading-edge devices used in this investigation were quite effective, further refinement would permit the attainment of higher lift coefficients at higher angles of attack.

### Full-Span Flaps

Effect of trailing-edge blowing and flap deflection at  $\alpha = 0^\circ$ . - The half-span flap blowing data of figure 6(a) showed that the most efficient gain in lift coefficient was obtained when the momentum coefficient was just sufficient to eliminate essentially the separated flow over highly deflected flaps. Further gains in  $C_L$  could be realized with increasing values of  $C_\mu$ , but the rate of increase was considerably reduced. It was believed that larger gains in lift could be obtained for a given amount of blowing air by directing the air, in excess of the amount required to produce essentially potential flow over the half-span flaps, to deflected outboard flaps or drooped ailerons.

The overall shape of the  $\Delta C_L - C_\mu$  curves at  $\alpha = 0^\circ$  (fig. 17(a)) is very similar to the curves obtained for half-span blowing except that the slopes of the curves for values of  $C_\mu$  above the knee are considerably larger than those obtained for the half-span blowing tests (fig. 6(a)). For a given value of  $C_\mu$ , blowing over full-span flaps also produced considerably larger increments of  $C_L$  than did the half-span blowing. The values of  $C_\mu$  (based on total wing area) required to produce unseparated flow over the full-span flaps (the knee of the curves) are greater than those required for half-span flaps because of the greater area treated.

A summary of the flap effectiveness at  $\alpha = 0^\circ$  as a function of flap angle is compared with potential lift values obtained by the method of reference 4 in figure 17(b). As in the case for half-span blowing, the potential flow lift values are in reasonable agreement with the experimental values obtained at the knee of the  $\Delta C_L - C_\mu$  curve.

Effect of trailing-edge blowing and flap deflection at angles of attack. - The results of tests conducted with full-span trailing-edge blowing applied over full-span deflected flaps in combination with the 0.60b/2 slat plus radius increase show that for the same  $C_\mu$  noted in the half-span tests, full-span blowing produced considerably larger values of  $C_L$  through the complete angle-of-attack range (fig. 16). Full-span blowing over outboard flaps (or ailerons) deflected  $30^\circ$  in combination with  $60^\circ$  deflected half-span flaps in general produced lift values (fig. 18) of the order of those obtained with full-span blowing over full-span flaps deflected  $50^\circ$  (fig. 16). Full-span trailing-edge blowing would appear to be the most efficient method for producing large values of  $C_L$  for a given value of  $C_\mu$ . However, for a highly swept wing, the apparent lift gains for a full-span flap arrangement may be totally compensated by the download on the tail required for trim as discussed in the following sections.

## PITCHING-MOMENT AND LONGITUDINAL TRIM CHARACTERISTICS

## Half-Span Flaps

Effect of trailing-edge blowing, flap deflection, and leading-edge devices.- The pitching-moment characteristics of the various configurations investigated at a given lift coefficient, as shown in figures 5 to 15, were relatively unaffected by the application of half-span trailing-edge blowing or increased rates of blowing.

The slopes of the pitching-moment curves with blowing applied were essentially linear and constant at a value of  $dC_m/dC_L$  of approximately -0.20 and indicated stable configurations through the lift range to maximum lift. For all configurations tested having blowing applied, unstable breaks in the pitching-moment curves occurred at  $C_{L_{max}}$ . This indicates the need for more effective outboard leading-edge treatment than was available on the present model.

Effect of leading-edge blowing at high angles of attack.- Leading-edge blowing (fig. 13) tended to produce larger values of negative pitching moment than did the no-leading-edge-blowing configurations; however, the magnitude of the unstable break at  $C_{L_{max}}$  was reduced. With further refinement of the leading-edge-blowing configuration, the unstable break in the pitching moments at  $C_{L_{max}}$  could probably be eliminated.

Effect of horizontal-tail deflection on longitudinal trim.- The static margin for the model was approximately 20 percent, with the assumed center of gravity, for all configurations. This static margin is considerably larger than would be required for a fighter aircraft of this type. A value of 8 to 10 percent would be a more reasonable figure which, if used, would result in higher values of maximum trimmed lift coefficient than those indicated in the present report. The tail incidence data presented in figure 19 for half-span flaps deflected  $60^\circ$  show that a normal tail installation would only be capable of trimming the model to maximum lift-coefficient values of the order of 1.1 for a blowing rate  $C_\mu$  of 0.099. For static-margin values of the order of 10 percent, however, a maximum trimmed lift coefficient of the order of 1.5 could be attained for a  $C_\mu$  of 0.099.

## Full-Span Flaps

Effect of trailing-edge blowing and flap deflection in combination with a full-span leading-edge device.- The pitching-moment characteristics



of the model for various combinations of full-span trailing-edge-flap deflections are adversely affected with the application of full-span trailing-edge blowing. With blowing applied, the negative pitching moments are increased over the no-blowing case, and the negative values continue to increase with either increased blowing rate or flap deflection (figs. 16 and 18). The negative pitching moments are approximately double those produced by blowing over half-span deflected flaps.

Effect of horizontal-tail deflection on longitudinal trim.- The negative pitching moments become so large with full-span blowing applied (figs. 16 and 18) that configurations having normal tail volume could not produce the negative lift required to trim the model. Tail incidence data for the configuration having full-span blowing applied over inboard flaps deflected  $60^\circ$  and outboard flaps (or ailerons) drooped  $30^\circ$  (fig. 20) show this to be the case. Even with the static margin reduced to about 10 percent, moderate values of  $C_{\mu}$  would produce negative pitching-moment values too large to be trimmed by a normal tail installation. Even if a tail could be designed to trim the large negative pitching moments, the associated loss in lift due to trim would probably negate most of the increase in lift that otherwise would have been obtained by blowing over full-span deflected flaps.

Because of the large negative pitching moments associated with the full-span blowing for an airplane of this sweep, trailing-edge blowing applied over half-span flaps is considered a more practical application.

Effect of trailing-edge blowing and flap deflection on the effective downwash.- The effective downwash characteristics obtained from tail loading data for the model having  $0.60b/2$  slats plus radius installed show that increasing the blowing rate over either the half- or the full-span flaps increases the effective downwash for the low angle-of-attack range (fig. 21); however, the effective downwash is considerably higher for half-span blowing than for full-span blowing. With blowing applied over either half- or full-span flaps the variation of the effective downwash with angle of attack is fairly uniform to an angle of attack of about  $12^\circ$  with the values of effective downwash decreasing rapidly for angles of attack above  $C_{l_{max}}$ .

## DRAG CHARACTERISTICS

### Half-Span Flaps

Effect of trailing-edge blowing, flap deflection, and leading-edge devices.- The drag characteristics of the model for the various half-span flap tests in general show that drag is increased with flap deflection

above  $40^\circ$  at a given lift coefficient and further increased when trailing-edge blowing is applied. (See figs. 5 to 15.) Increasing the rate of blowing, for the  $C_\mu$  range covered, apparently had little effect on the drag characteristics. Leading-edge devices in general produced a decrease in drag in the moderate to high angle-of-attack range for the no-blowing and low  $C_\mu$  tests; however, for the higher  $C_\mu$  range the installation of leading-edge devices had no apparent effect on drag.

Effect of leading-edge blowing at high angles of attack.- Leading-edge blowing in combination with the full-span leading-edge-radius increase (fig. 13) produced essentially the same effects on the drag characteristics as did the other leading-edge devices, except for the case where  $C_{\mu TE} = 0$ . For  $C_{\mu TE} = 0$ , leading-edge blowing also reduced the drag values for a given lift coefficient in the low angle-of-attack range.

#### Full-Span Flaps

Effect of trailing-edge blowing and flap deflection in combination with a full-span leading-edge device.- In general, the drag characteristics of the model for the various combinations of flap deflections used (ailerons used as flaps) show that for the condition of  $C_\mu = 0$ , increasing flap angle produced an increase in the drag (fig. 16). With full-span blowing applied over flaps deflected  $40^\circ$  and  $50^\circ$ , however, the drag is decreased and continues to decrease with increased blowing rate. For full-span flap angles of  $60^\circ$  increased blowing rates at a given lift coefficient seemed to have negligible effects on the drag characteristics. The reduction in drag due to blowing over flaps deflected  $40^\circ$  and  $50^\circ$  is probably associated with the reduced model angle of attack for a given lift coefficient and the more uniform span loading for the full-span-blowing configuration (noted in ref. 5) resulting in considerably reduced values of induced drag. The drag characteristics of the model with blowing applied over  $60^\circ$  deflected half-span flaps and  $30^\circ$  drooped ailerons (fig. 18) are about the same as those experienced with trailing-edge blowing applied over the full-span  $50^\circ$  deflected-flaps configuration.

#### LIFT-DRAG RATIO

#### Half-Span Flaps

Effect of trailing-edge blowing and flap deflection in combination with a full-span leading-edge device.- The variations of  $L/D$  with  $C_L$

for the model with half-span flaps deflected  $40^\circ$ ,  $50^\circ$ , and  $60^\circ$  (fig. 22) in general show that  $L/D$  decreased with increasing flap angle, and for lift coefficients below approximately 1.2 (except for the  $40^\circ$  flap configuration),  $L/D$  was decreased when blowing was applied. The values of  $L/D$  for flap angles of  $50^\circ$  and  $60^\circ$  with blowing applied are essentially constant over a wide lift-coefficient range to  $C_{l_{max}}$ .

### Full-Span Flaps

Effect of trailing-edge blowing and flap deflection in combination with a full-span leading-edge device.- The variations of  $L/D$  with  $C_L$  for the model with full-span flaps deflected  $40^\circ$ ,  $50^\circ$ , and  $60^\circ$  (fig. 23) show that increasing flap angle decreased the value of  $L/D$  for a given value of  $C_L$  either with or without full-span blowing applied. For comparable lift coefficients, blowing at a value of  $C_\mu$  of 0.027 had very little effect on the values of  $L/D$ . Increasing the rate of trailing-edge blowing to a value of  $C_\mu$  of 0.099, however, considerably increased the values of  $L/D$  for flap angles of  $40^\circ$  and  $50^\circ$ . For a flap angle of  $60^\circ$  the increased blowing rate did not increase the values of  $L/D$ ; however, the increased blowing rate did extend the lift range of the  $60^\circ$  flapped configuration without any appreciable loss in  $L/D$ .

### LATERAL CONTROL

#### Half-Span Flaps

Effect of trailing-edge blowing on the aileron effectiveness.- It is interesting to note that blowing applied over half-span flaps deflected  $60^\circ$  provided improved aileron effectiveness through the angle-of-attack range investigated for a wide range of aileron deflection angles (fig. 24(a)). At high angles of attack and control deflection the rolling power of the ailerons was approximately doubled. These improved aileron characteristics are probably associated with the entrainment of a portion of the normally spanwise boundary-layer flow toward the half-span flaps thus partially cleaning up the flow over the outboard portion of the wing.

Effect of leading-edge blowing on the aileron effectiveness.- It was noted from flow studies made for the configuration having leading-edge blowing applied (fig. 15) that the marked improvement in the flow over the outboard portion of the wing should produce very good aileron effectiveness characteristics. As shown in figure 25, leading-edge blowing increased the aileron effectiveness through the deflection and angle-of-attack range investigated, and produced a twofold increase in rolling moment at high angles of attack for  $C_{\mu_{LE}}$  of 0.025.

Effect of trailing-edge blowing on the yawing characteristics.- For the model configuration having half-span flaps deflected  $60^\circ$ , with or without half-span blowing applied, only small adverse yawing tendencies are noted with differential aileron deflection for angles of attack through  $11^\circ$  (fig. 24(c)). Also the yawing characteristics were relatively unaffected by increased blowing over the flaps for the  $C_{\mu}$  range investigated.

Effect of leading-edge blowing on the yawing characteristics.- In general the adverse yaw with aileron deflection was small for the configuration having leading-edge blowing over the outboard 38 percent of the wing span (fig. 25) and about the same order of magnitude as that obtained for the half-span flap tests without leading-edge blowing (fig. 24(c)).

### Full-Span Flaps

Effect of trailing-edge blowing on the aileron effectiveness.- For an aileron deflection range of approximately  $20^\circ$  to  $60^\circ$ , full-span trailing-edge blowing over  $60^\circ$  deflected half-span flaps and  $30^\circ$  initially drooped ailerons (fig. 24(b)) provided aileron effectiveness, for comparable blowing rates, greater than those obtained for the normal aileron with blowing applied only over the  $60^\circ$  deflected half-span flaps (fig. 24(a)). The aileron effectiveness was considerably reduced, however, at the higher deflection angles for the lower blowing rate investigated.

Effect of trailing-edge blowing on the yawing characteristics.- Full-span trailing-edge blowing over  $60^\circ$  deflected half-span flaps and  $30^\circ$  initially drooped ailerons produced severe adverse yaw with differential aileron deflection which increased with increased rate of blowing (fig. 24(d)).

### CONCLUSIONS

An investigation of boundary-layer control by blowing over trailing-edge flaps in conjunction with several leading-edge-flow control devices, including leading-edge blowing on a  $49^\circ$  swept wing-body-tail model yielded the following results:

1. Boundary-layer control by blowing over trailing-edge flaps deflected to angles up to  $60^\circ$  results in flap lift increments approximately equal to values predicted by potential flow theory for moderate values of blowing momentum coefficient. Additional lift increases can

be obtained by increasing the blowing momentum rate, but the rate of lift increase with momentum coefficient is much reduced after the flap separation is eliminated.

2. For a given momentum coefficient, full-span flap blowing provides larger lift increments, untrimmed, than obtained with half-span flap blowing; however, for a highly swept wing, pitching moments for the full-span case become so large that longitudinal trim cannot be obtained with a normal tail volume.

3. Effective full-span leading-edge-stall control devices are required with trailing-edge blowing applied over flaps if the lift gains obtained at low angles of attack are to be maintained through the normal angle-of-attack range and the maximum lift coefficient increased.

4. Blowing from a rearward directed slot located outboard in the wing upper surface very near the leading edge provided effective leading-edge-stall control when combined with leading-edge-radius increase.

5. Blowing over half-span flaps has little effect on the model pitching moments or longitudinal stability at a given lift coefficient up to maximum lift. Blowing over full-span flaps greatly increased the diving moments as compared with those obtained for the half-span flap configuration.

6. Blowing over the inboard half-span flap or blowing applied outboard at the wing leading edge provides marked improvement in the aileron effectiveness of outboard located ailerons.

Langley Aeronautical Laboratory,  
National Advisory Committee for Aeronautics,  
Langley Field, Va., May 1, 1956.

~~REFERENCES~~

1. Bamber, Millard J.: Wind Tunnel Tests on Airfoil Boundary Layer Control Using a Backward-Opening Slot. NACA Rep. 385, 1931.
2. Schvier, W.: Lift Increases by Blowing Out Air, Tests on Airfoil of 12 Percent Thickness, Using Various Types of Flap. NACA TM 1148, 1947.
3. Lyon, R. M., and Hills, R.: Lift Increase by Boundary Layer Control. B.A. Dept. Note - Wind Tunnels No. 391, British R.A.E., May 1939.
4. DeYoung, John: Theoretical Symmetric Span Loading Due to Flap Deflection for Wings of Arbitrary Plan Form at Subsonic Speeds. NACA Rep. 1071, 1952. (Supersedes NACA TN 2278.)
5. Whittle, Edward F., Jr., and McLemore, H. Clyde: Aerodynamic Characteristics and Pressure Distributions of a 6-Percent-Thick 49° Sweptback Wing With Blowing Over Half-Span and Full-Span Flaps. NACA RM L55F02, 1955.

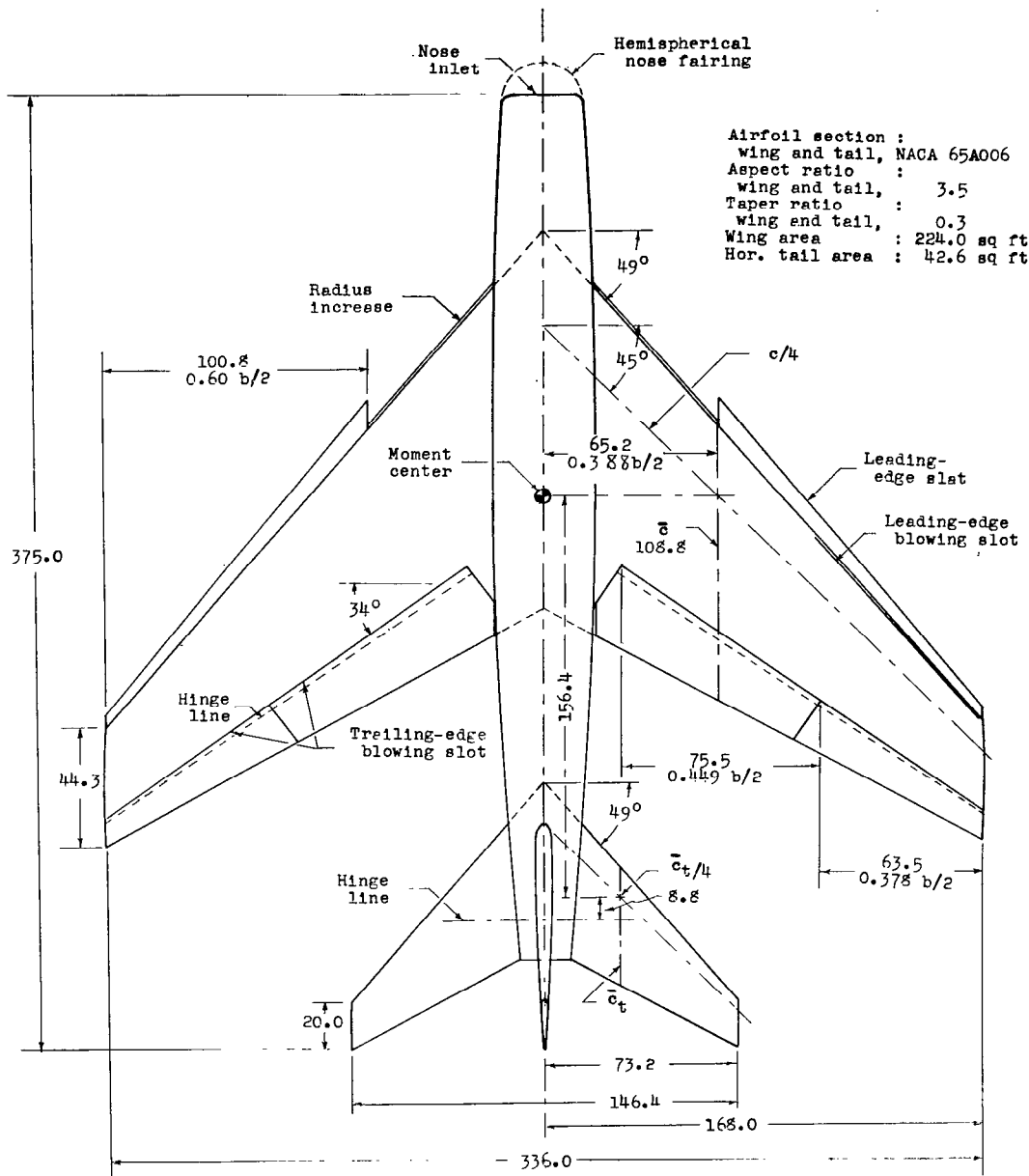
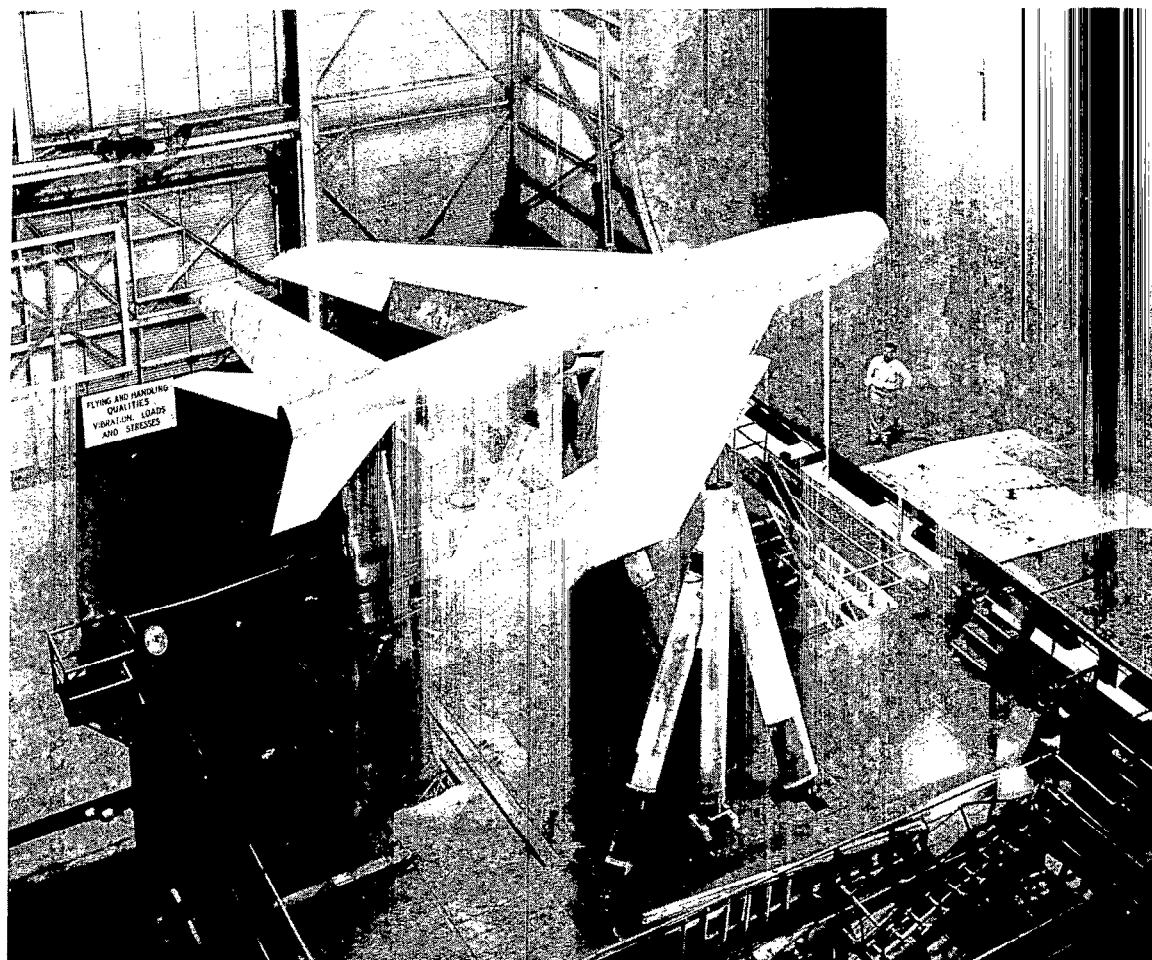


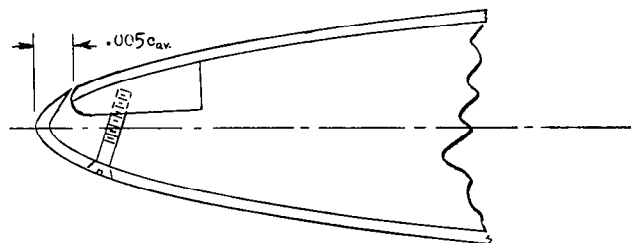
Figure 1.- Geometrical characteristics of the model. All dimensions are in inches.



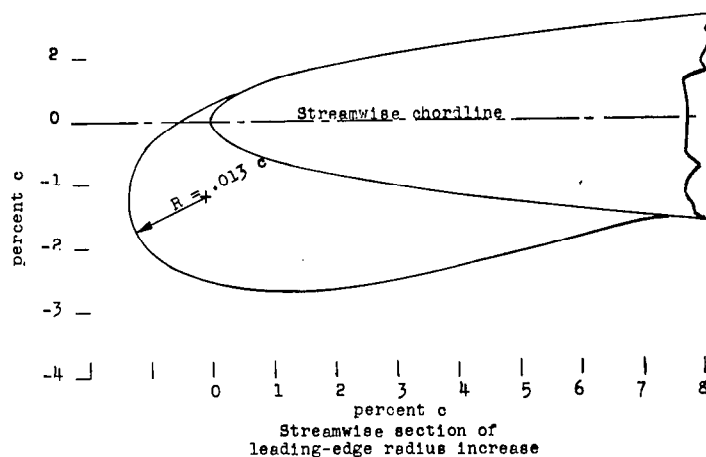
L-88820

Figure 2.- Three-quarter rear view of the model mounted for tests in the Langley full-scale tunnel. 0.60b/2 slat plus radius increase installed;  $\delta_f = 60^\circ$ ;  $\delta_a = 30^\circ$ ;  $i_t = 0^\circ$ .

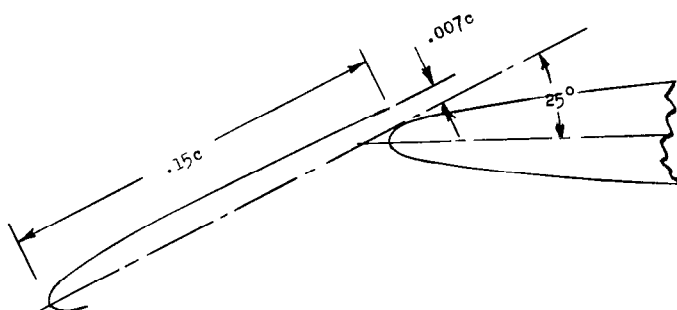




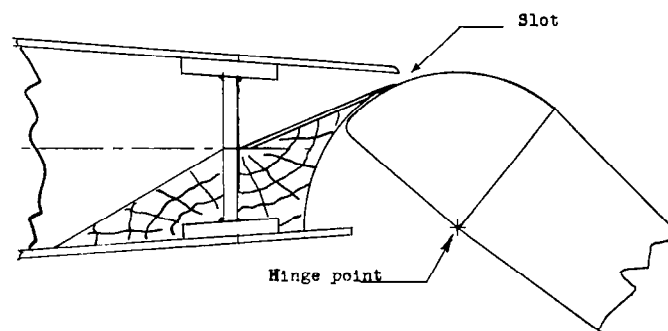
Streamwise section of  
leading-edge blowing slot



Streamwise section of  
leading-edge radius increase



Streamwise section of  
leading-edge slat



Flap or aileron and  
trailing-edge blowing slot  
(section normal to hinge line)

Figure 3.- Sectional views of various leading-edge devices and leading-  
and trailing-edge blowing slots.

CONFIDENTIAL

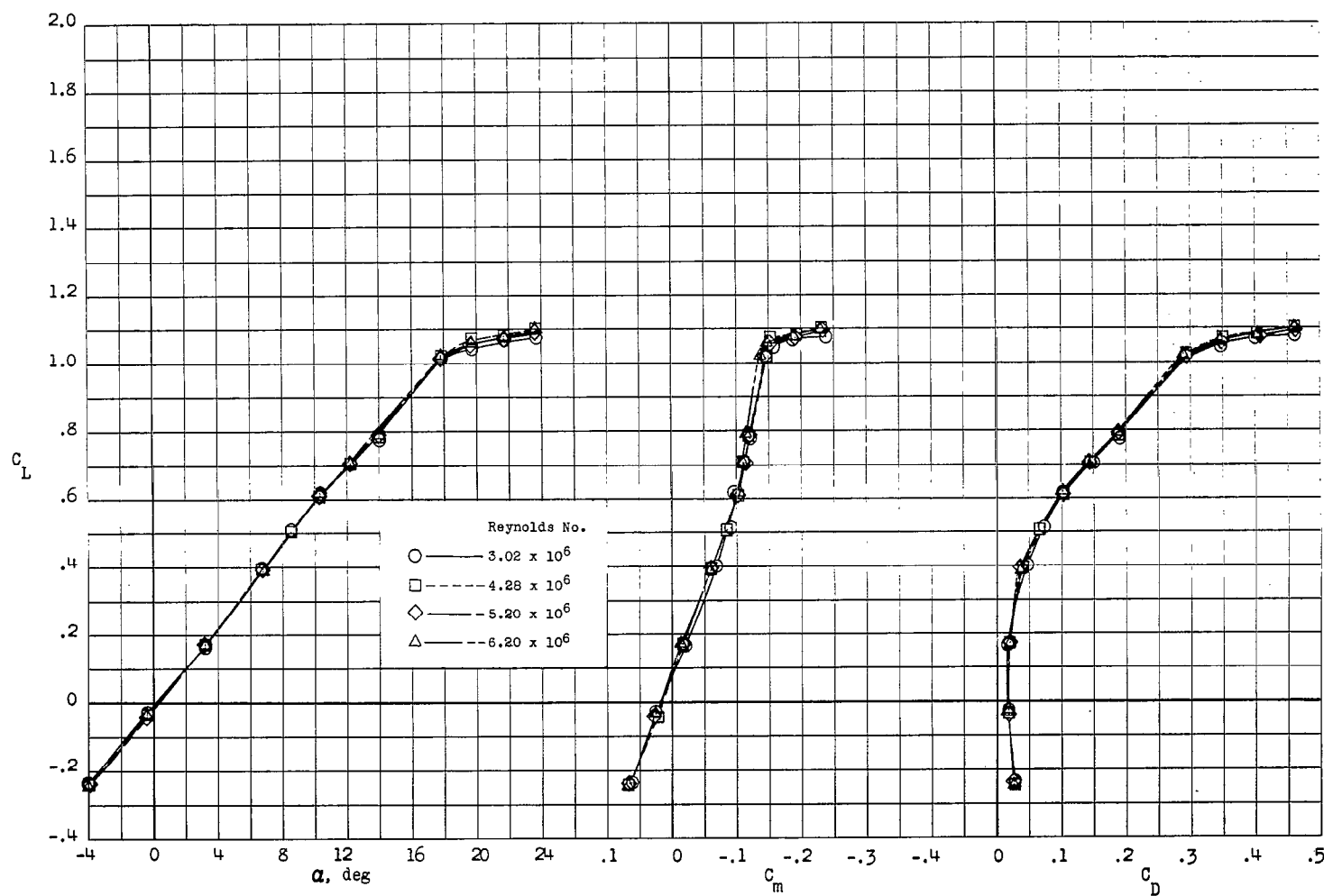


Figure 4.- Effect of Reynolds number on the aerodynamic characteristics of the basic wing configuration.  $\delta_f = 0^\circ$ ;  $\delta_a = 0^\circ$ ;  $i_t = 0^\circ$ .

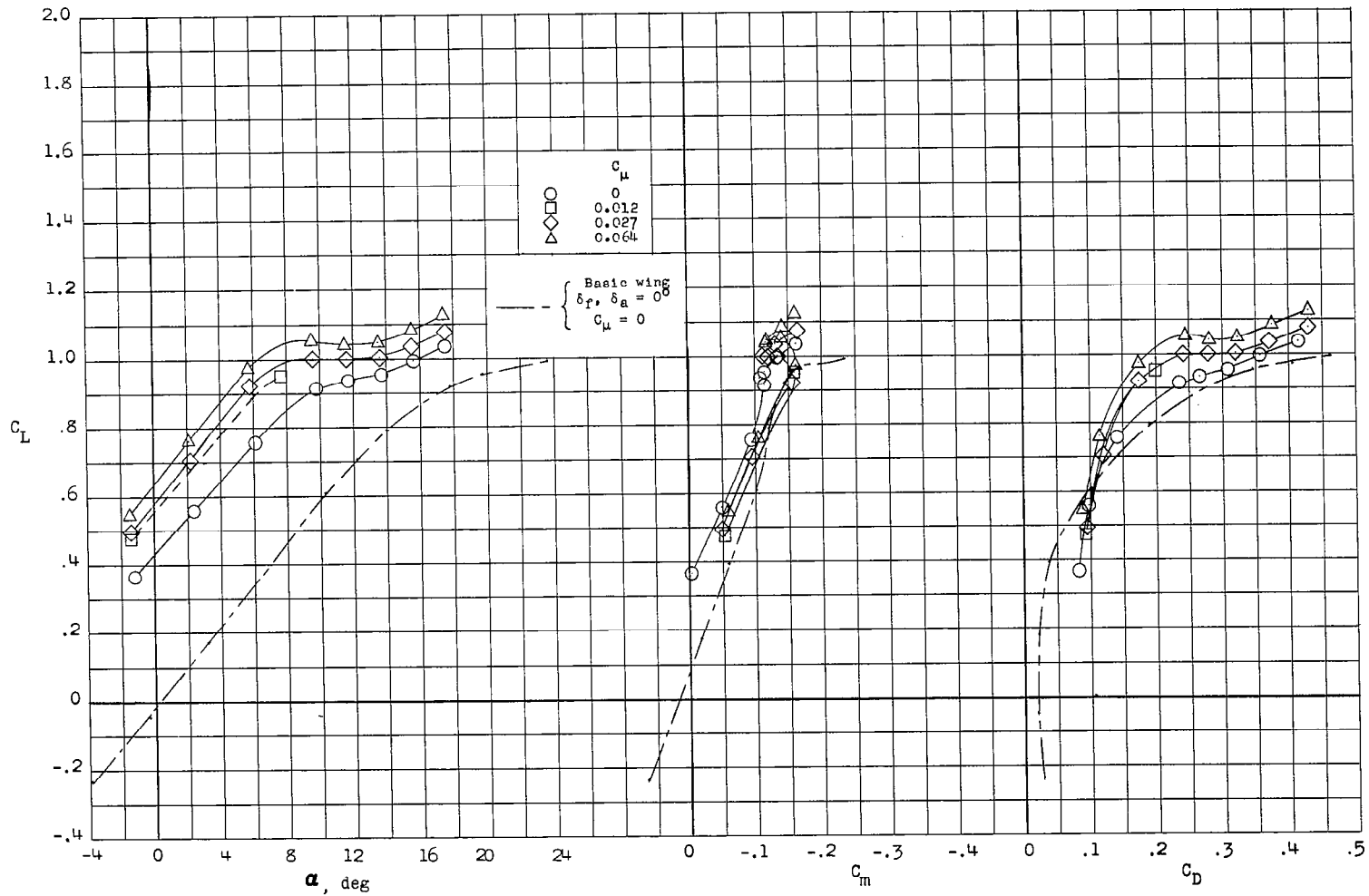
(a)  $\delta_f = 40^\circ$ .

Figure 5.- Effect of trailing-edge blowing over half-span flaps on the aerodynamic characteristics of the basic leading-edge configuration.  
 $\delta_a = 0^\circ$ ;  $i_t = 0^\circ$ .

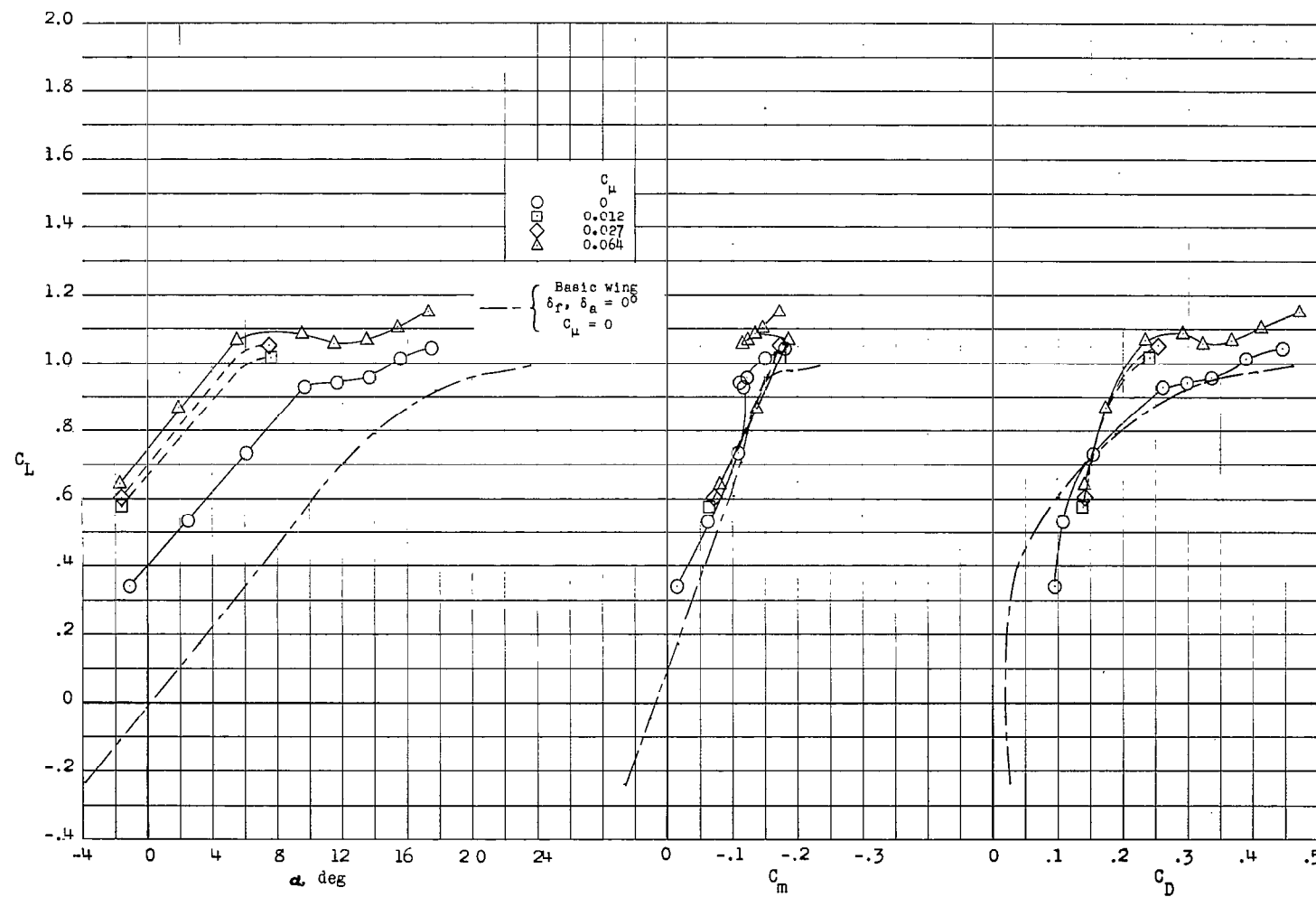
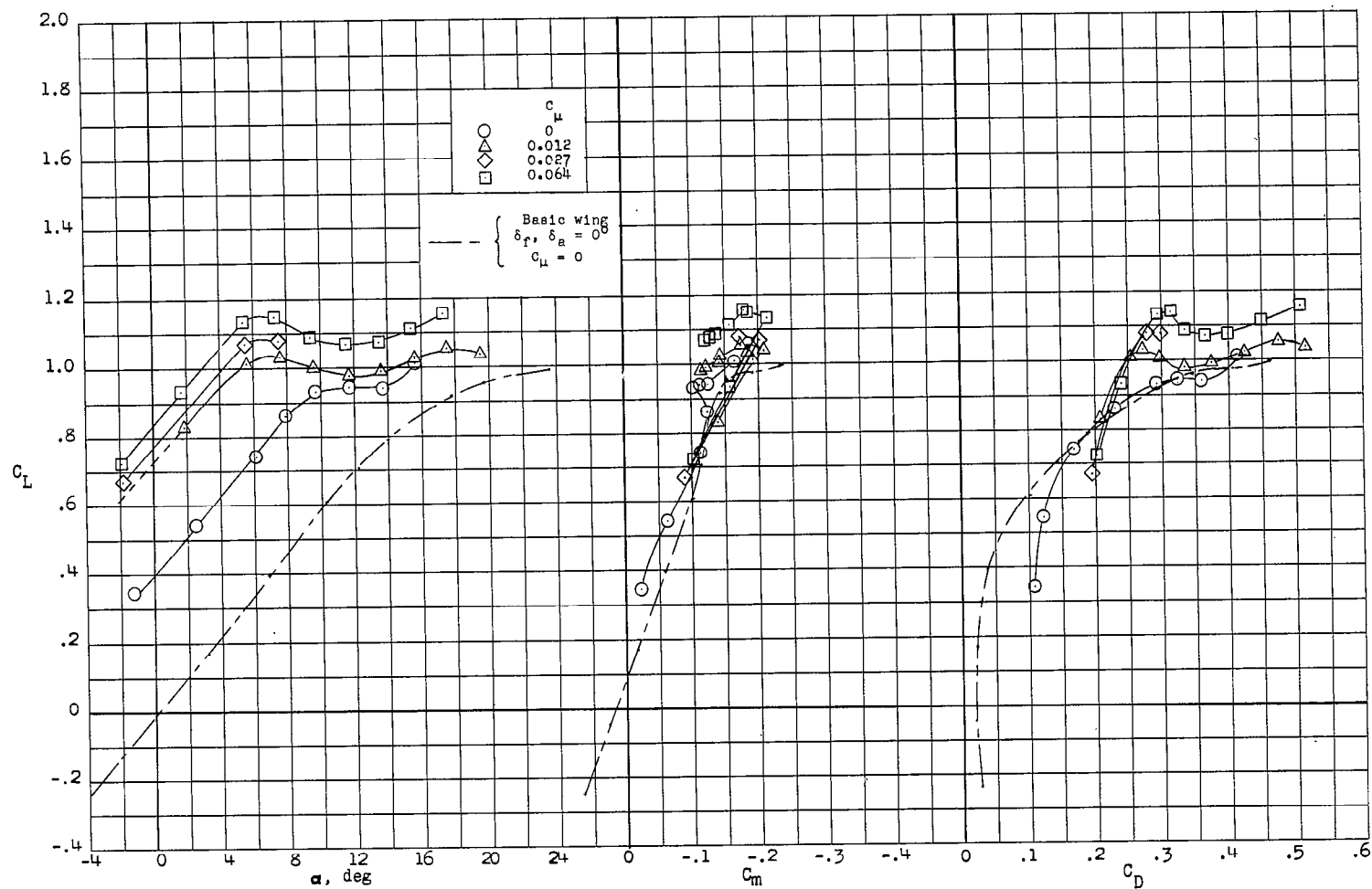
(b)  $\delta_f = 50^\circ$ .

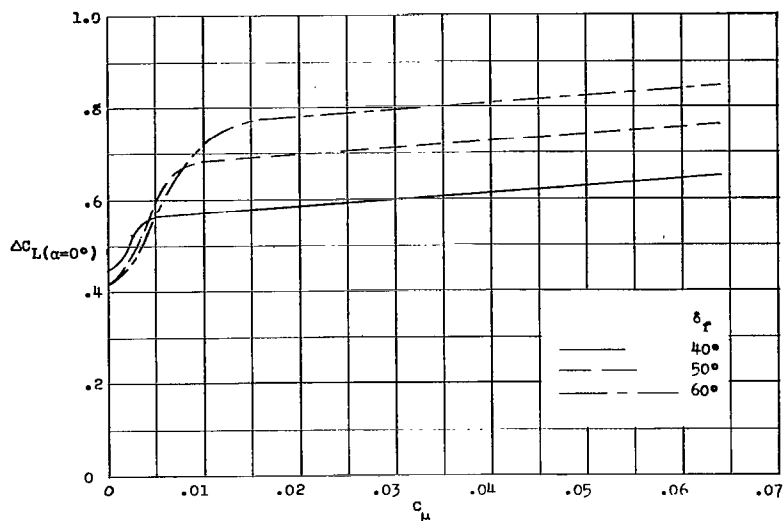
Figure 5.- Continued.



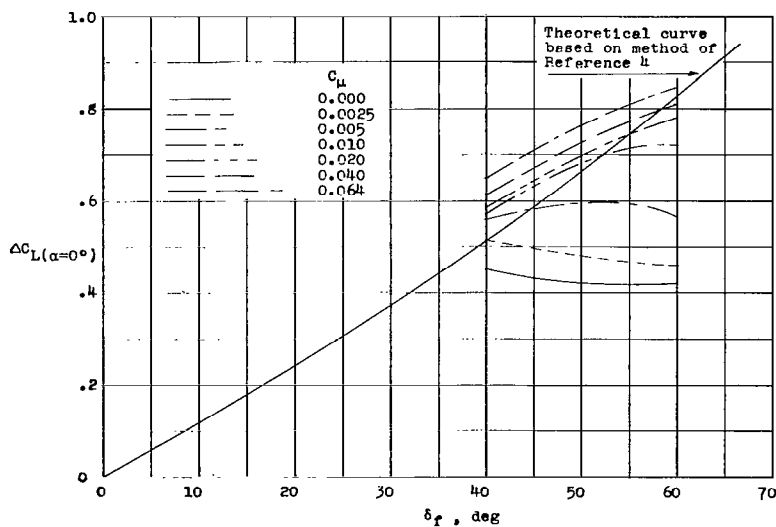
(c)  $\delta_F = 60^\circ$ .

Figure 5.- Concluded.

CONFIDENTIAL



(a) Variation of  $\Delta C_L$  with momentum coefficient for several flap angles.



(b) Variation of  $\Delta C_L$  with flap angle for several momentum coefficients.

Figure 6.- Variation of  $\Delta C_L(\alpha=0^\circ)$  with momentum coefficient and half-span flap-deflection angles of  $40^\circ$ ,  $50^\circ$ , and  $60^\circ$ . Basic leading-edge configuration;  $\delta_a = 0^\circ$ .

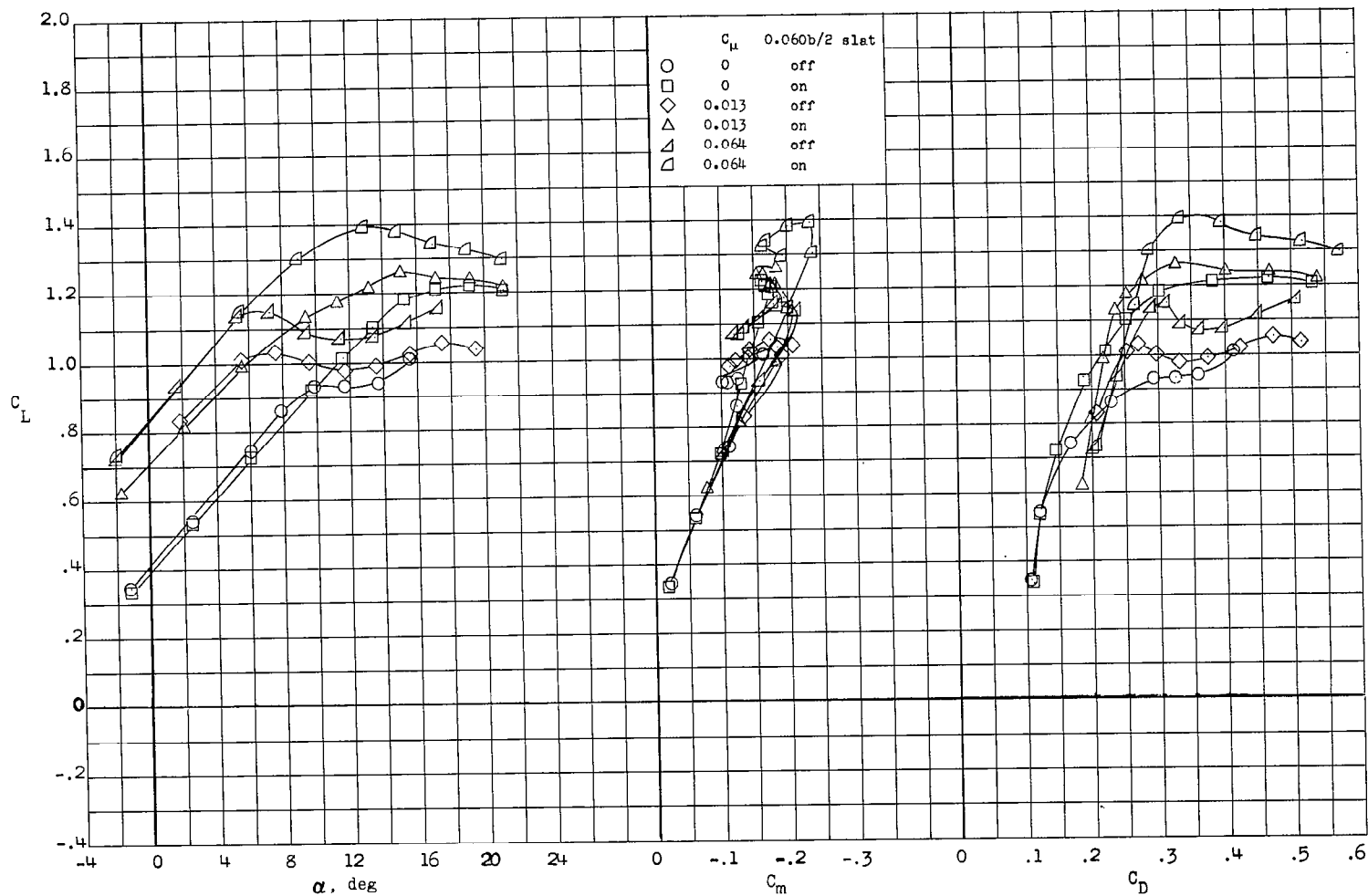


Figure 7.- Effect on the aerodynamic characteristics of installing 0.60b/2 slats with and without trailing-edge blowing over half-span flaps deflected 60°.  $\delta_a = 0^\circ$ ;  $i_t = 0^\circ$ .

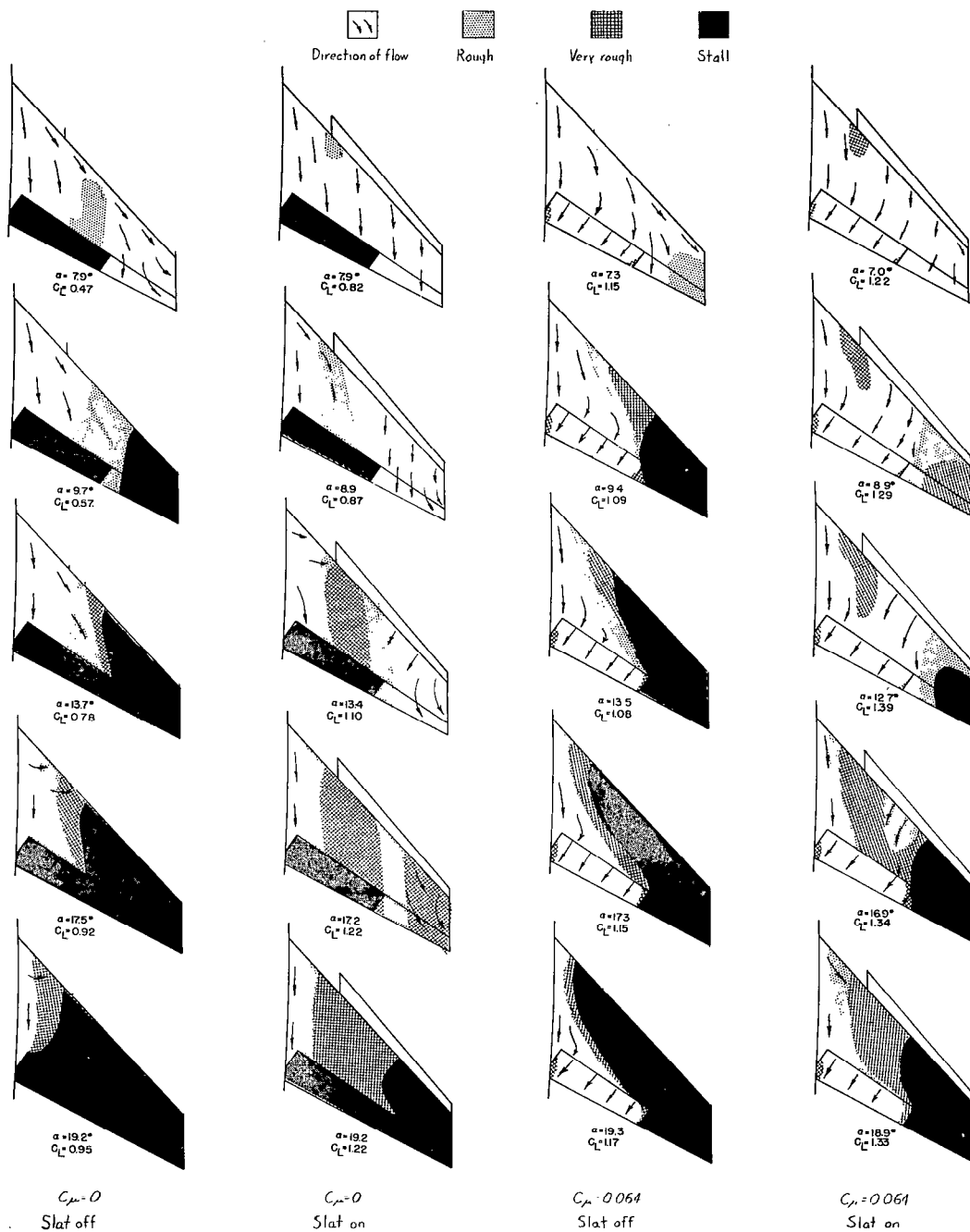


Figure 8.- Effect of installing 0.60b/2 slats with and without trailing-edge blowing over half-span flaps.  $\delta_f = 60^\circ$ ;  $\delta_a = 0^\circ$ .



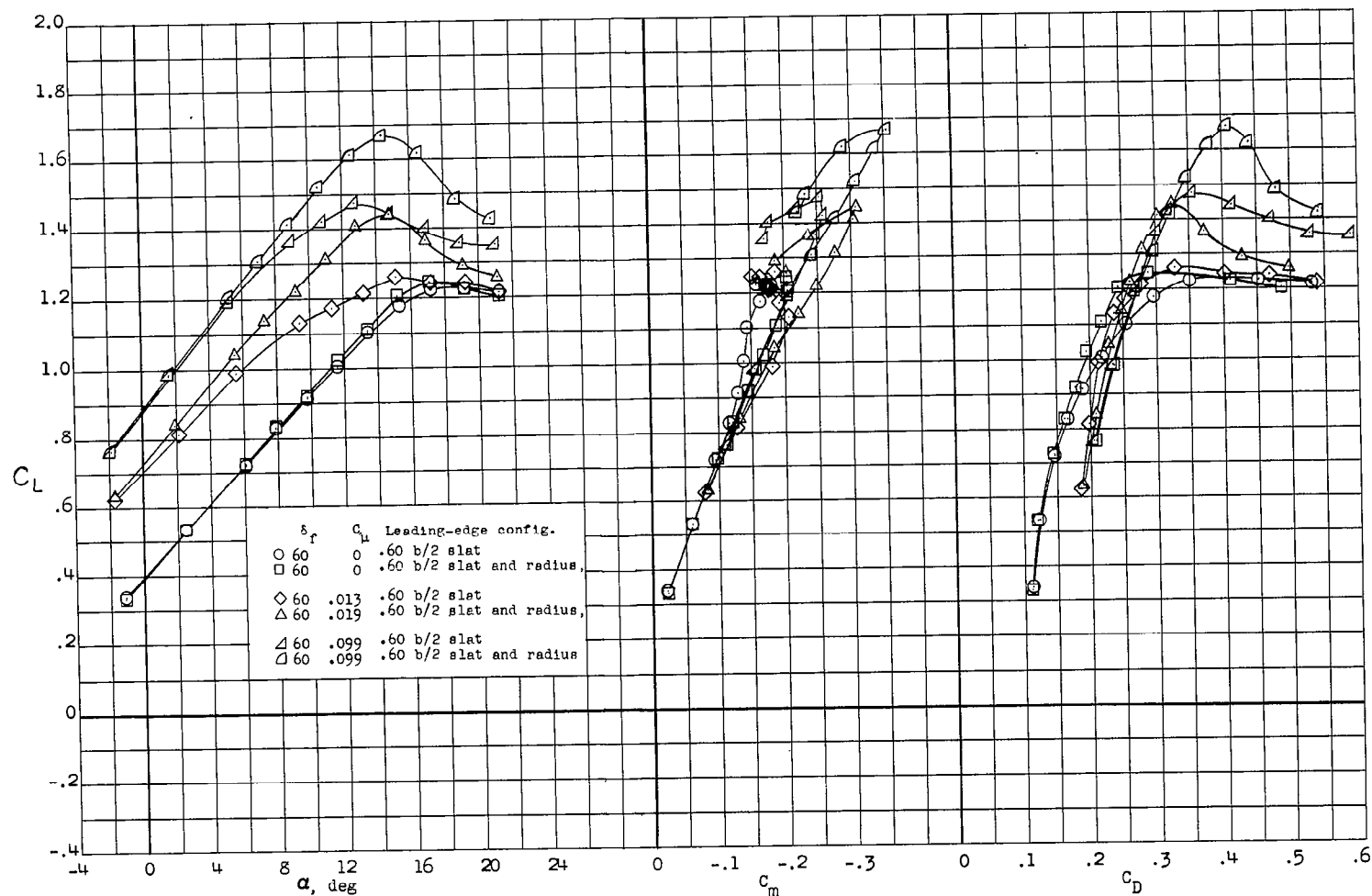


Figure 9.- Effect of adding leading-edge-radius increase inboard of 0.60b/2 slat with and without trailing-edge blowing over half-span flaps.  $\delta_a = 0^\circ$ ;  $i_t = 0^\circ$ .

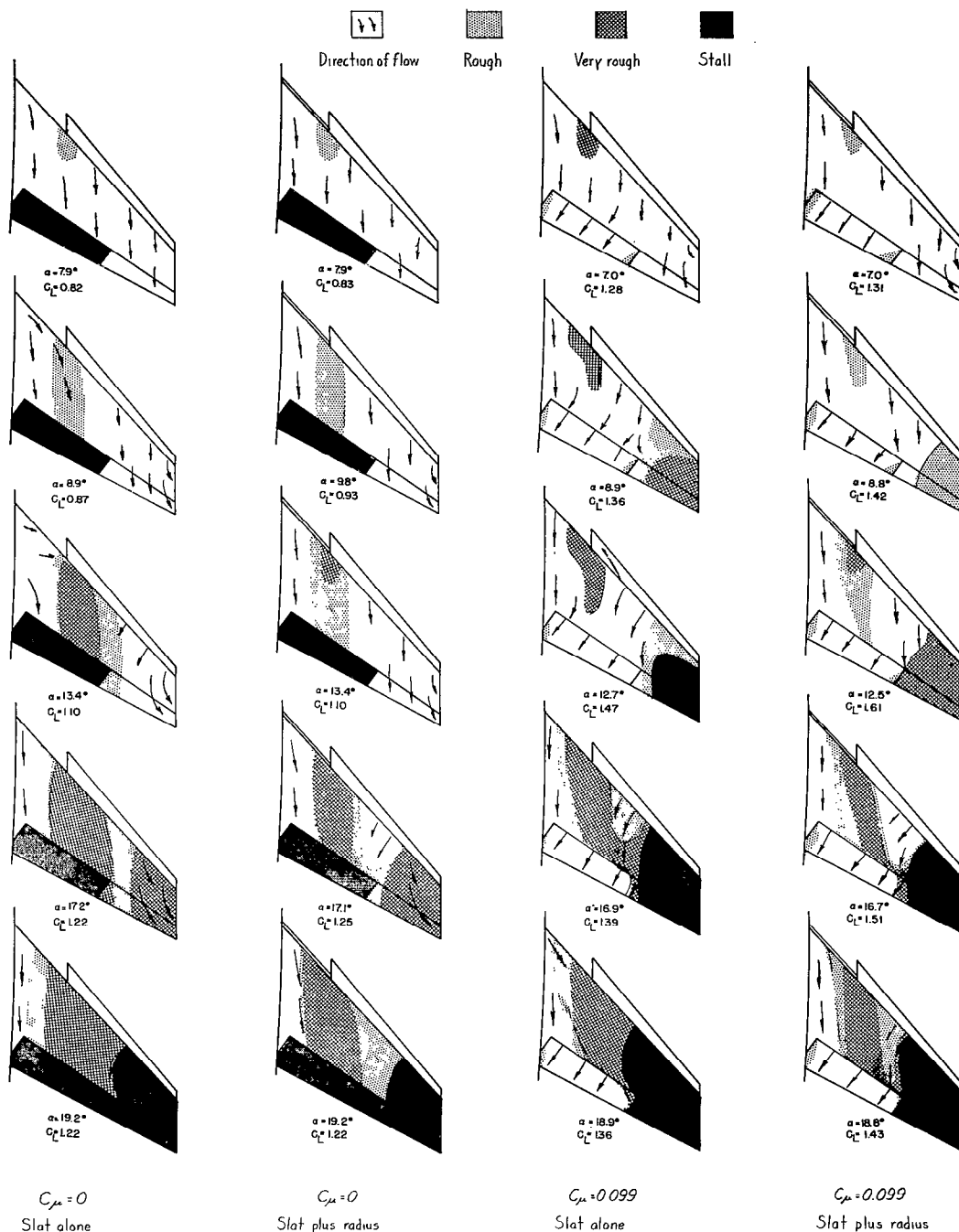


Figure 10.- Effect of installing leading-edge radius increase to portion of wing inboard of  $0.60b/2$  slats with and without trailing-edge blowing over half-span flaps.  $\delta_f = 60^\circ$ ;  $\delta_a = 0^\circ$ .

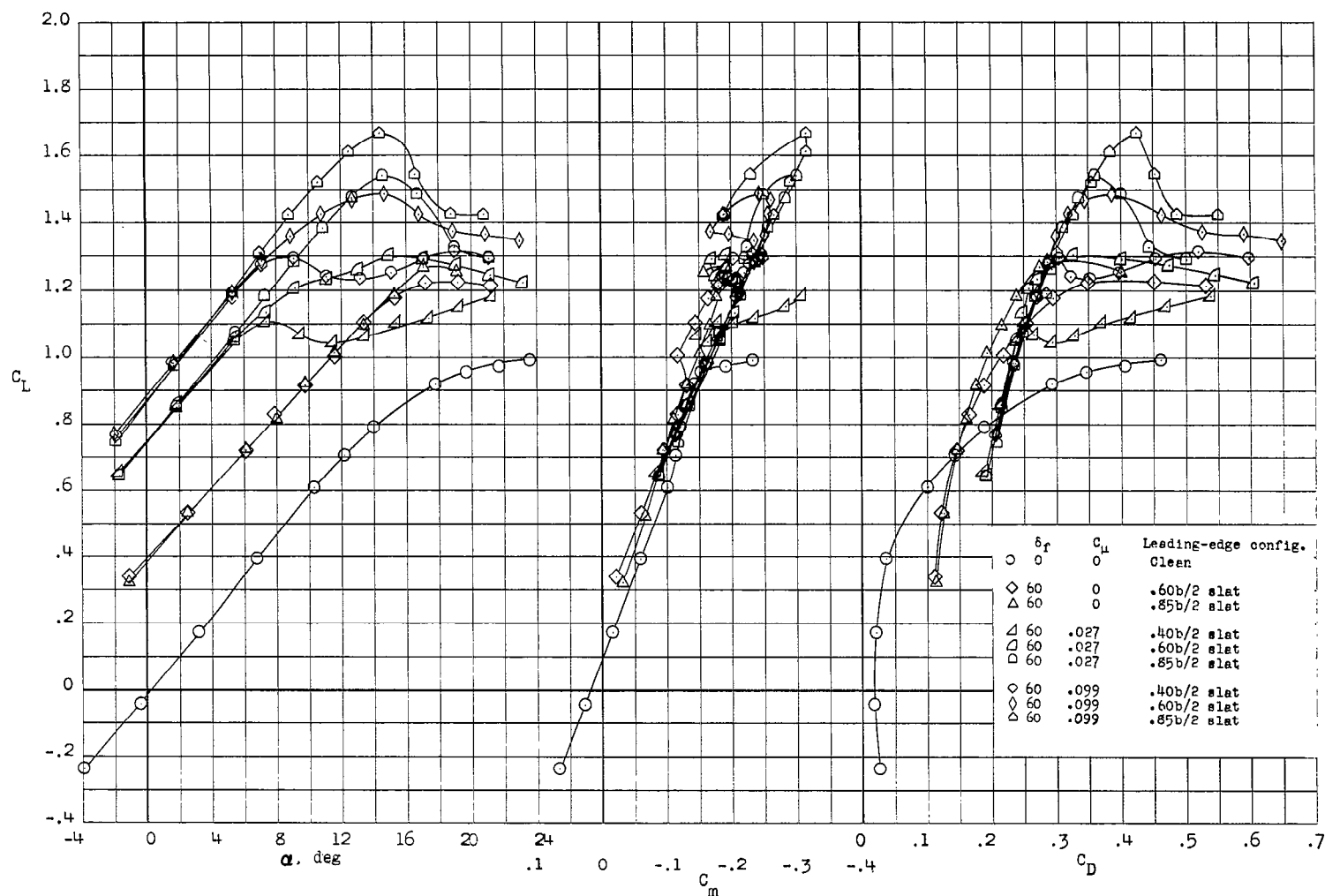


Figure 11.- Effect on the aerodynamic characteristics of increasing the slat span with and without trailing-edge blowing over half-span flaps.  $\delta_a = 0^\circ$ ;  $i_t = 0^\circ$ .

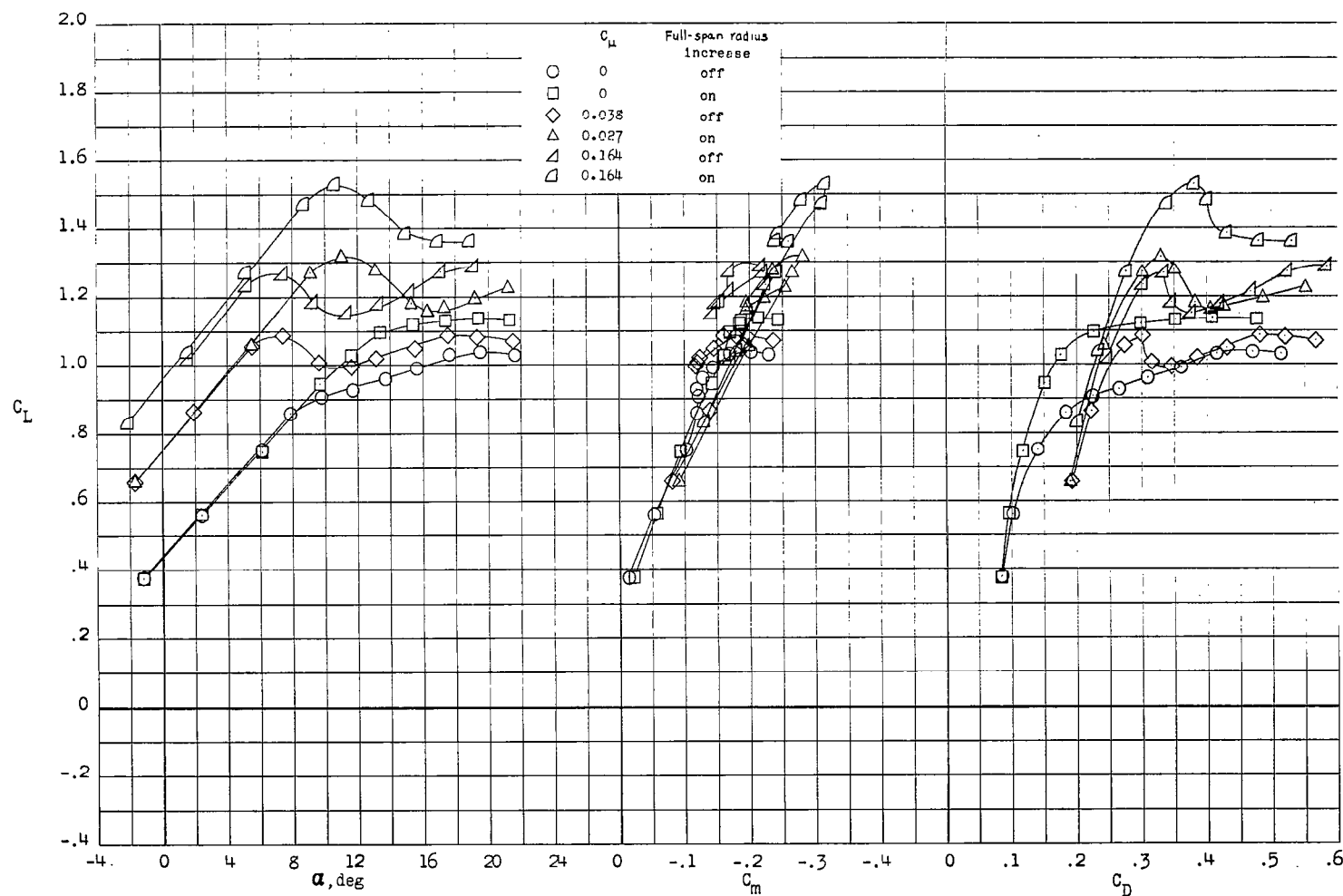


Figure 12.- Effect on the aerodynamic characteristics of installing full-span leading-edge radius increase with and without trailing-edge blowing over half-span flaps.  $\delta_f = 60^\circ$ ;  $\delta_a = 0^\circ$ ;  $i_t = 0^\circ$ .

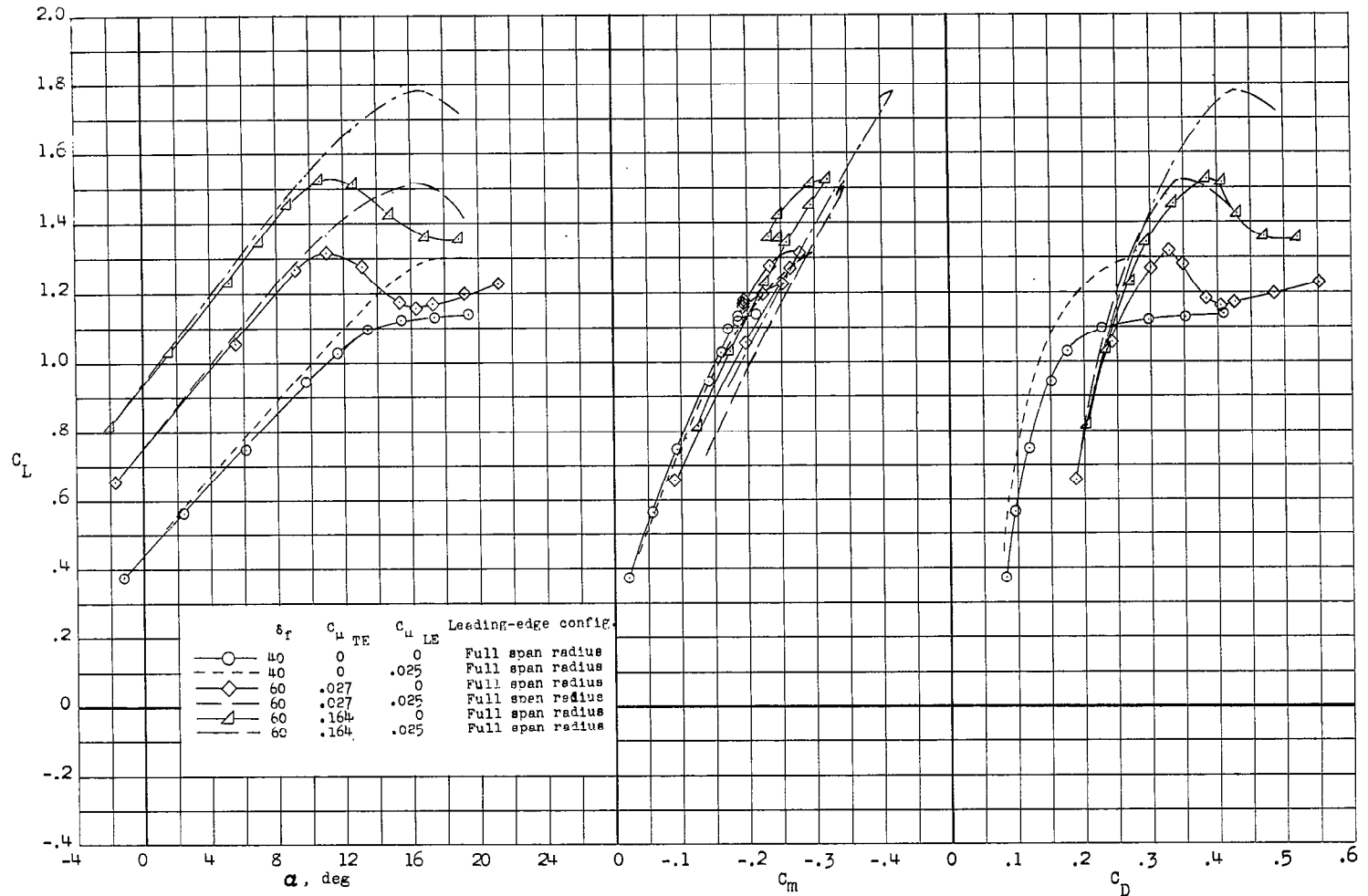


Figure 13.- Effect of leading-edge blowing in combination with full-span leading-edge radius increase on the aerodynamic characteristics with and without trailing-edge blowing over half-span flaps.  $\delta_a = 0^\circ$ ;  $i_t = 0^\circ$ .

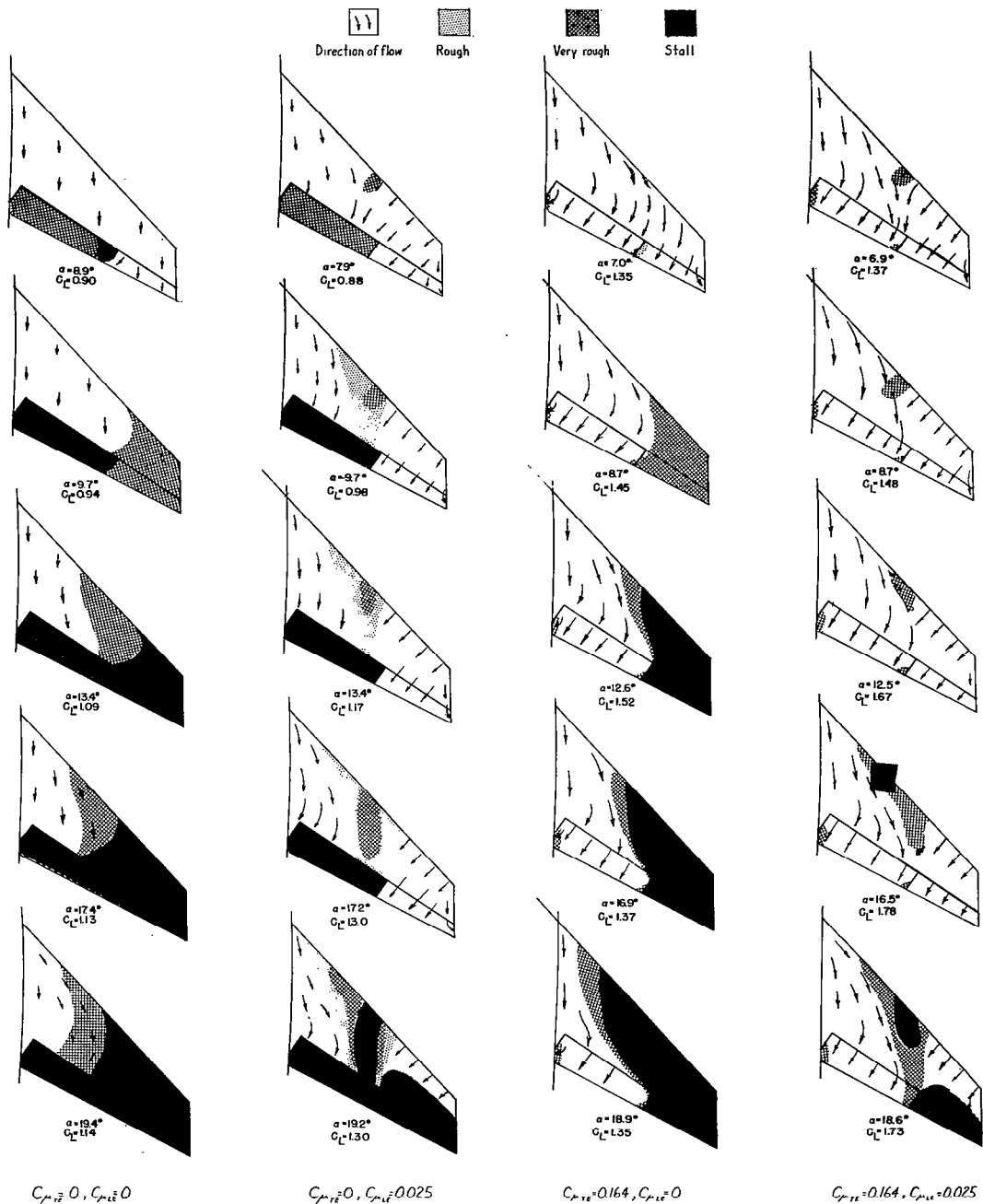
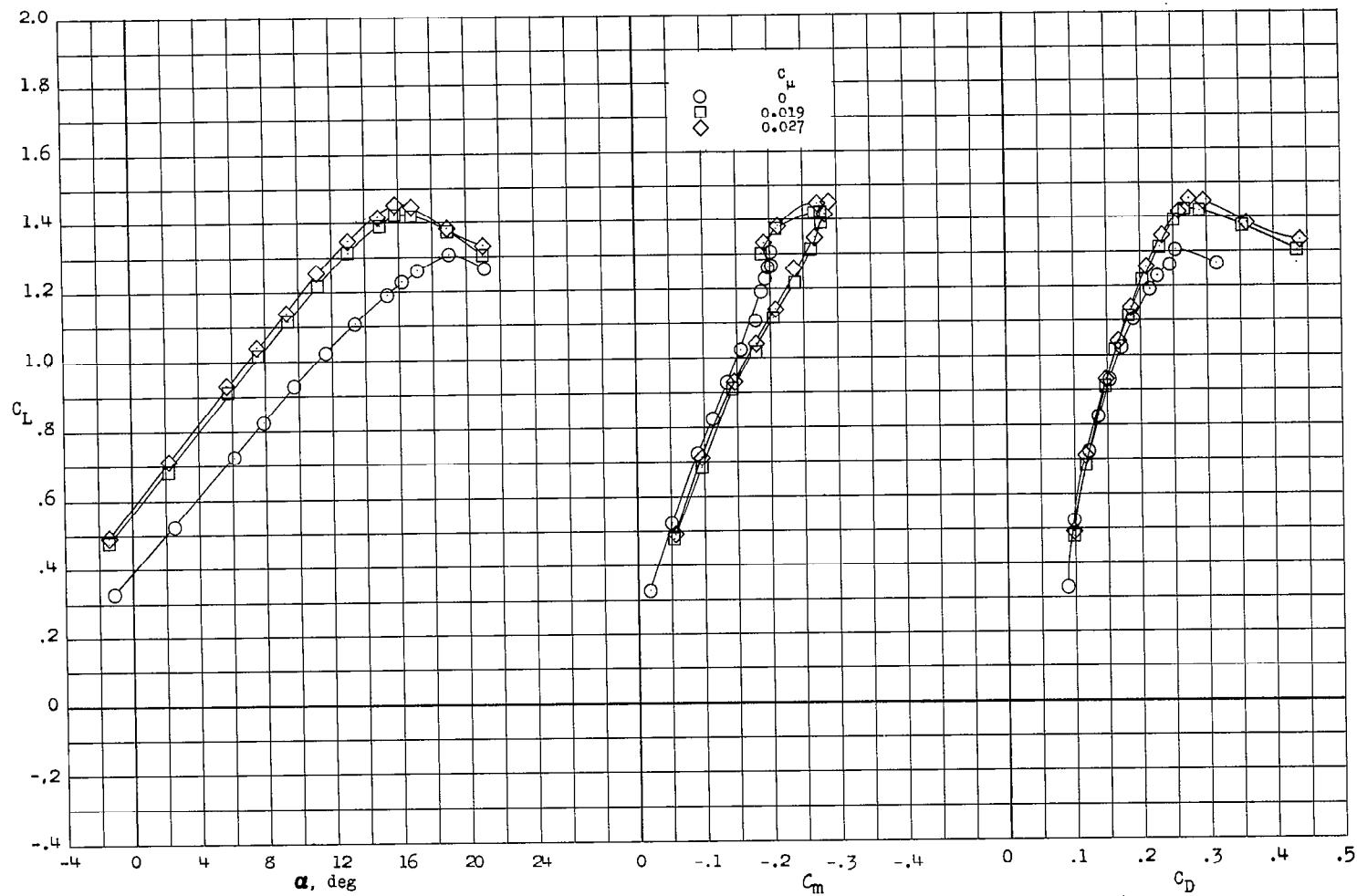
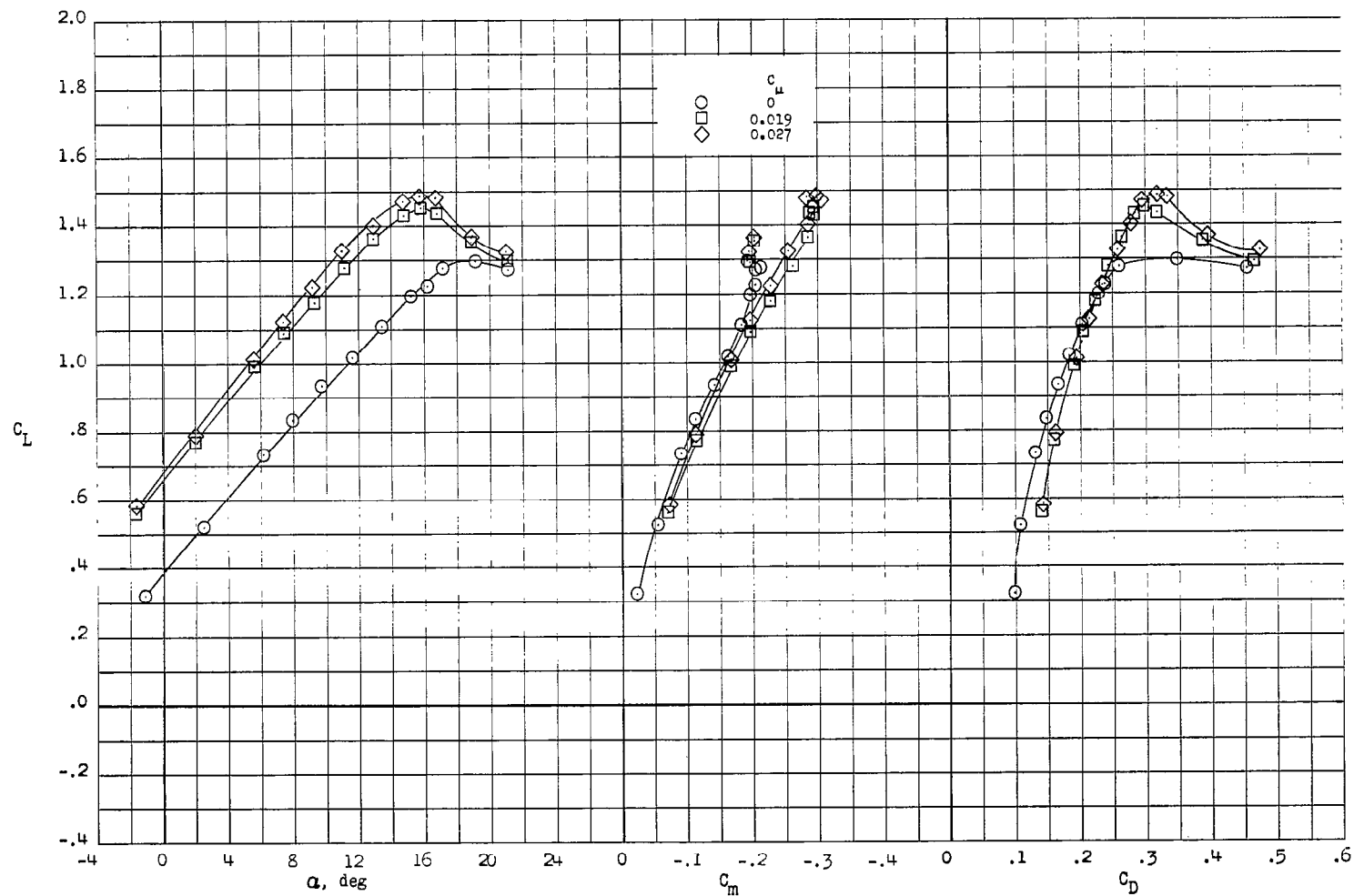


Figure 14.- Effect of leading-edge blowing in combination with the full-span leading-edge-radius increase with and without trailing-edge blowing applied over half-span flaps.  $\delta_f = 60^\circ$ ;  $\delta_a = 0^\circ$ .



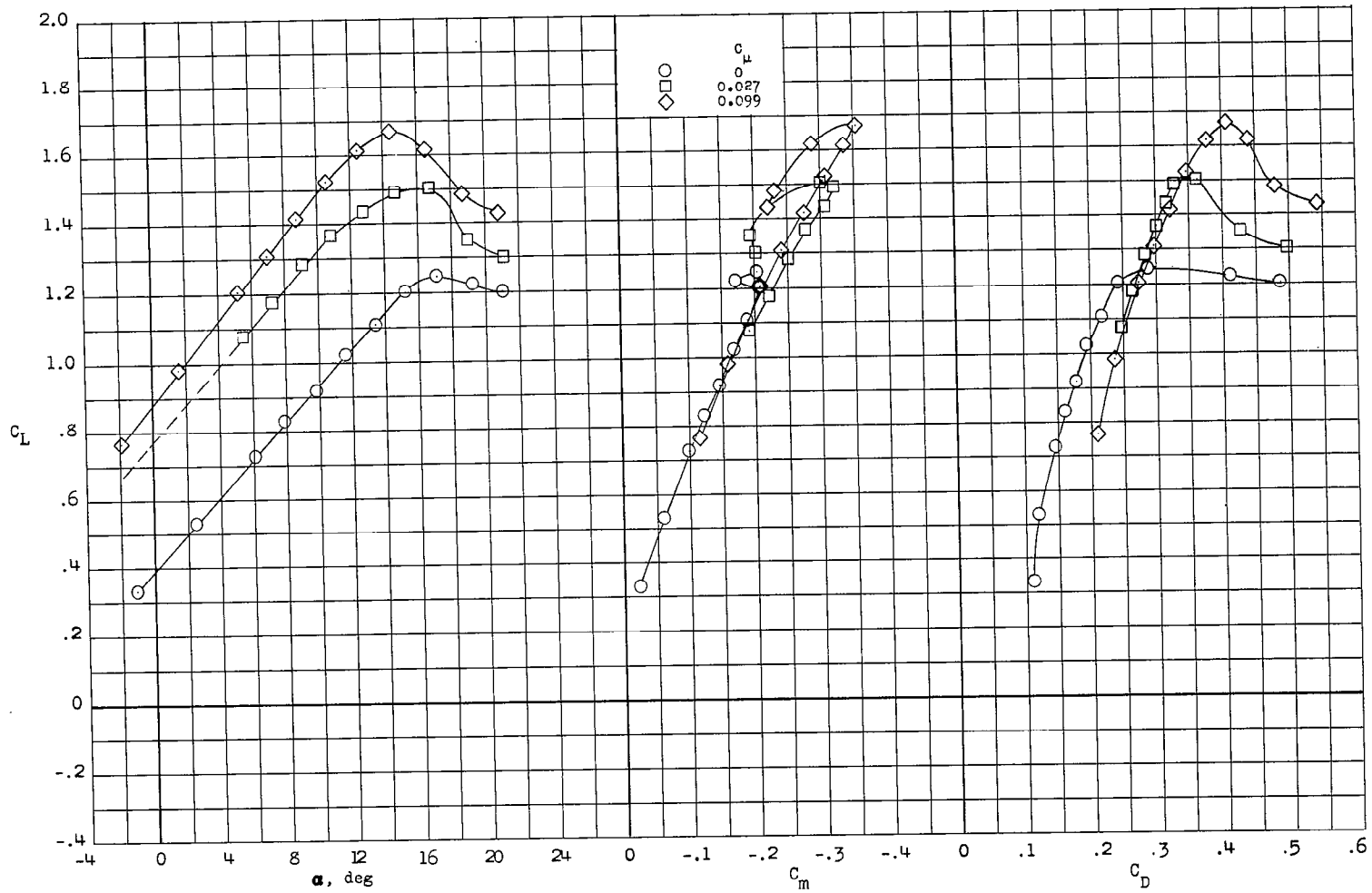
(a)  $\delta_f = 40^\circ$ .

Figure 15.- Effect of trailing-edge blowing over half-span flaps on the aerodynamic characteristics with  $0.60b/2$  slat plus radius increase installed.  $\delta_a = 0^\circ$ ;  $i_t = 0^\circ$ .



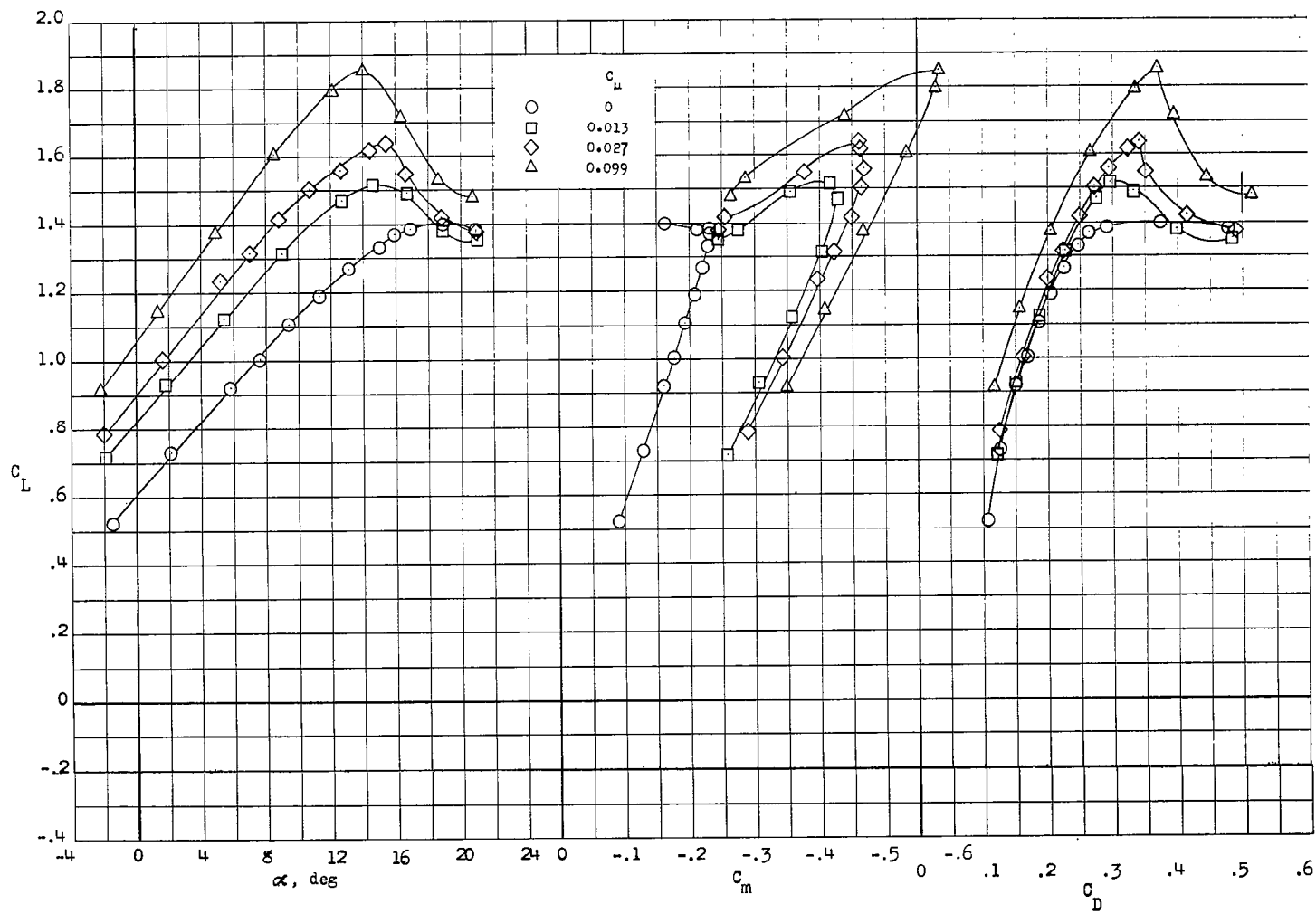
(b)  $\delta_F = 50^\circ$ .  
Figure 15.- Continued.





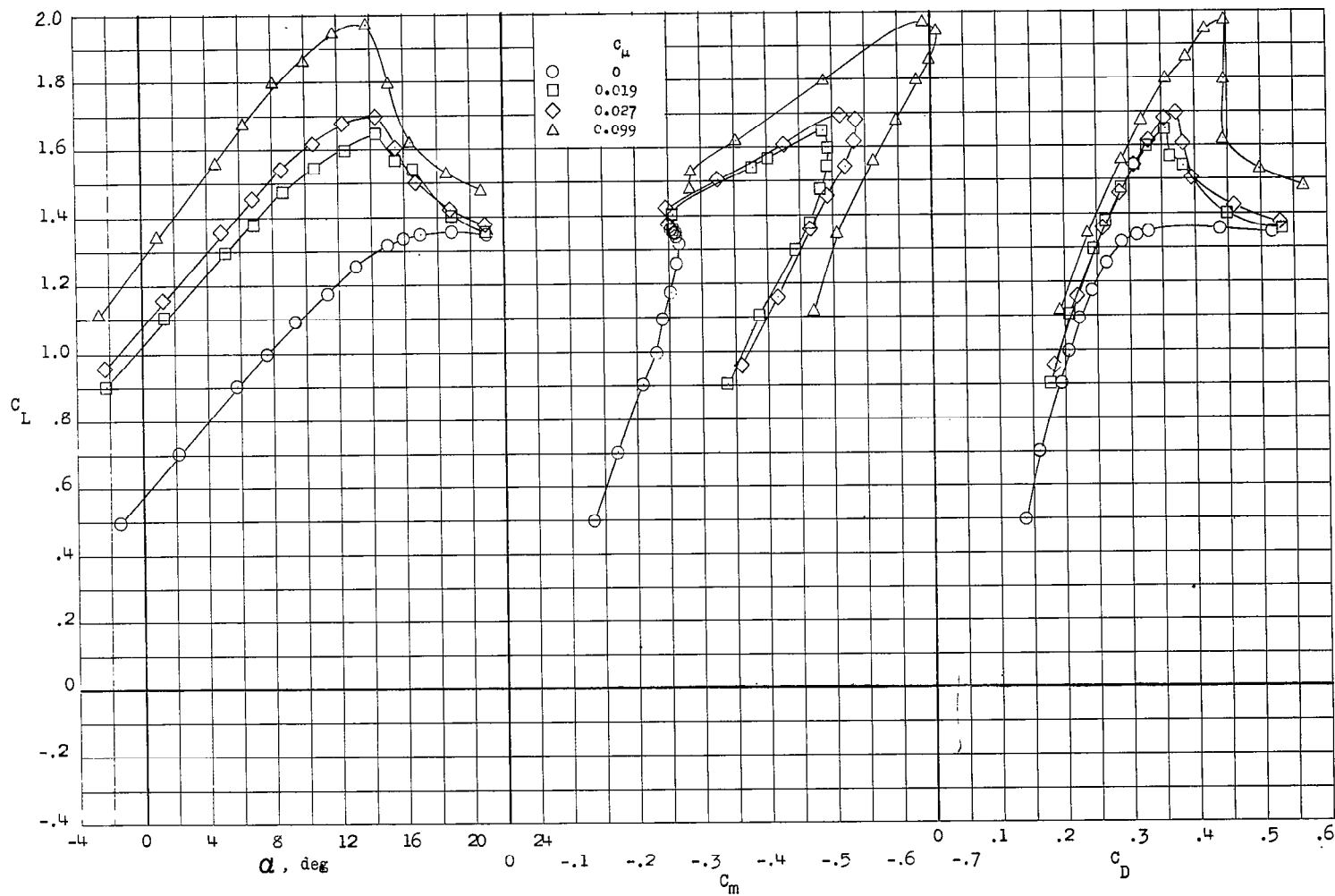
(c)  $\delta_f = 60^\circ$ .

Figure 15.- Concluded.



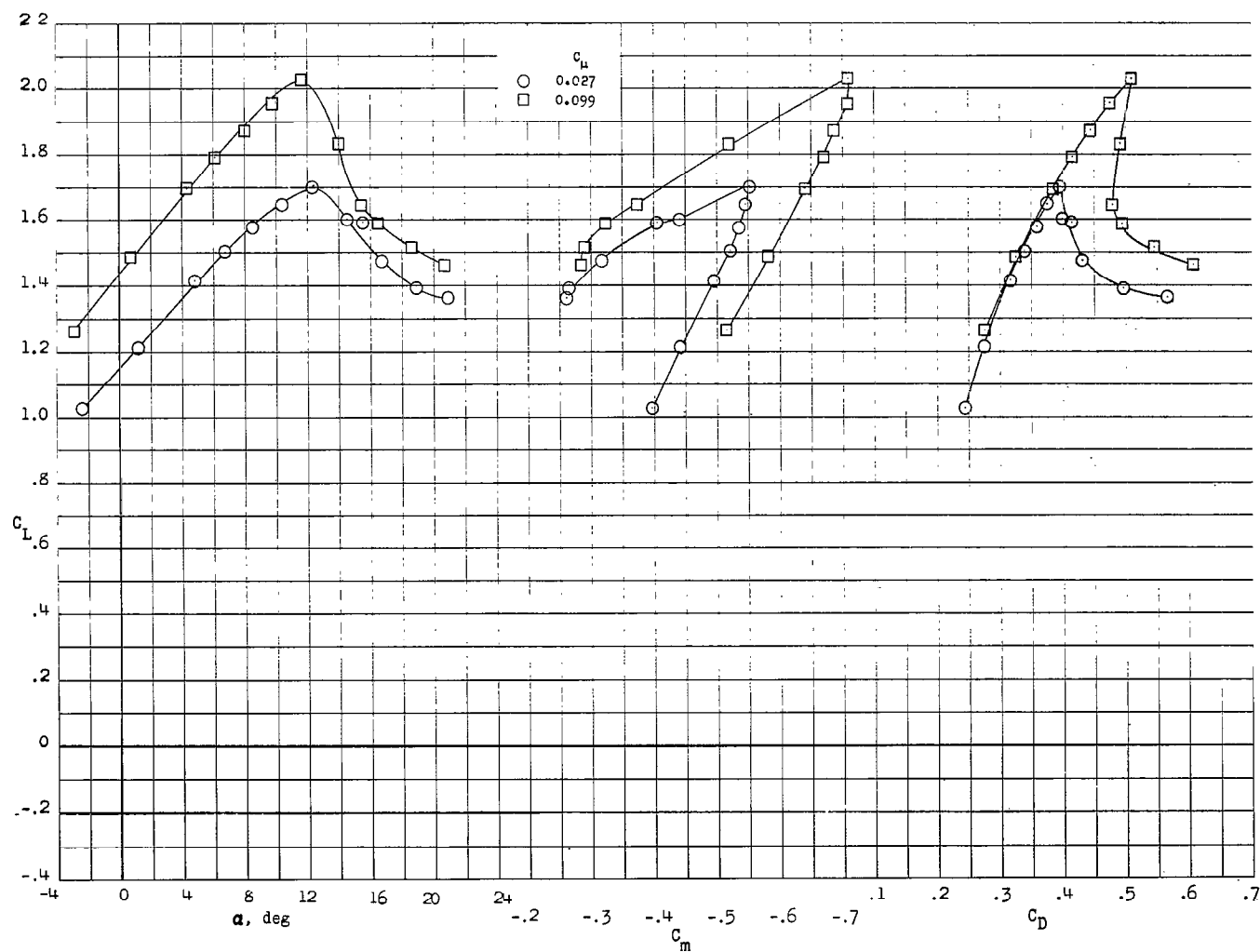
(a)  $\delta_f, \delta_a = 40^\circ$ .

Figure 16.- Effect on the aerodynamic characteristics of deflecting full-span flaps with and without full-span trailing-edge blowing.  
0.60b/2 slat plus radius increase installed;  $i_t = 0^\circ$ .



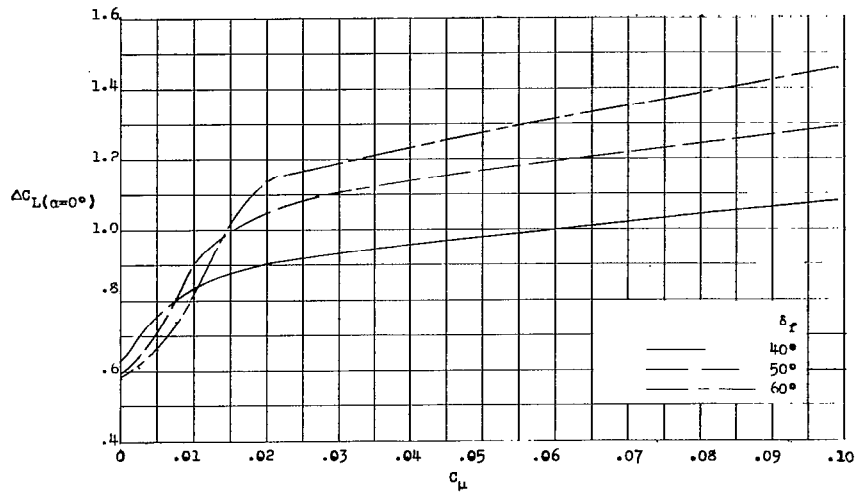
(b)  $\delta_f, \delta_a = 50^\circ$ .

Figure 16.- Continued.

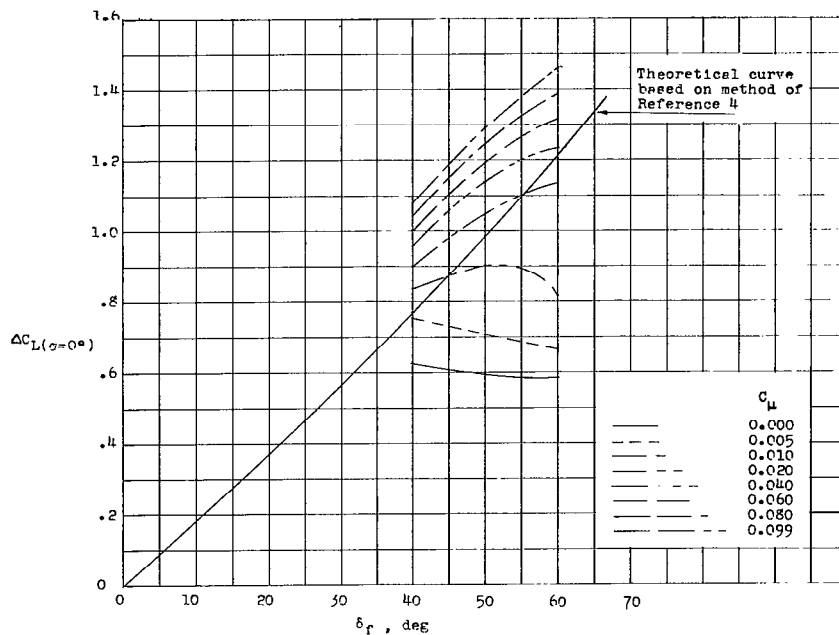


(c)  $\delta_f, \delta_a = 60^\circ$ .

Figure 16.- Concluded.



(a) Variation of  $\Delta C_L$  with momentum coefficient for several flap angles.



(b) Variation of  $\Delta C_L$  with flap angle.

Figure 17.- Variation of  $\Delta C_L(\alpha=0^\circ)$  with full-span momentum coefficient and full-span flap-deflection angles of 40°, 50°, and 60°. 0.60b/2 slat plus radius increase installed.

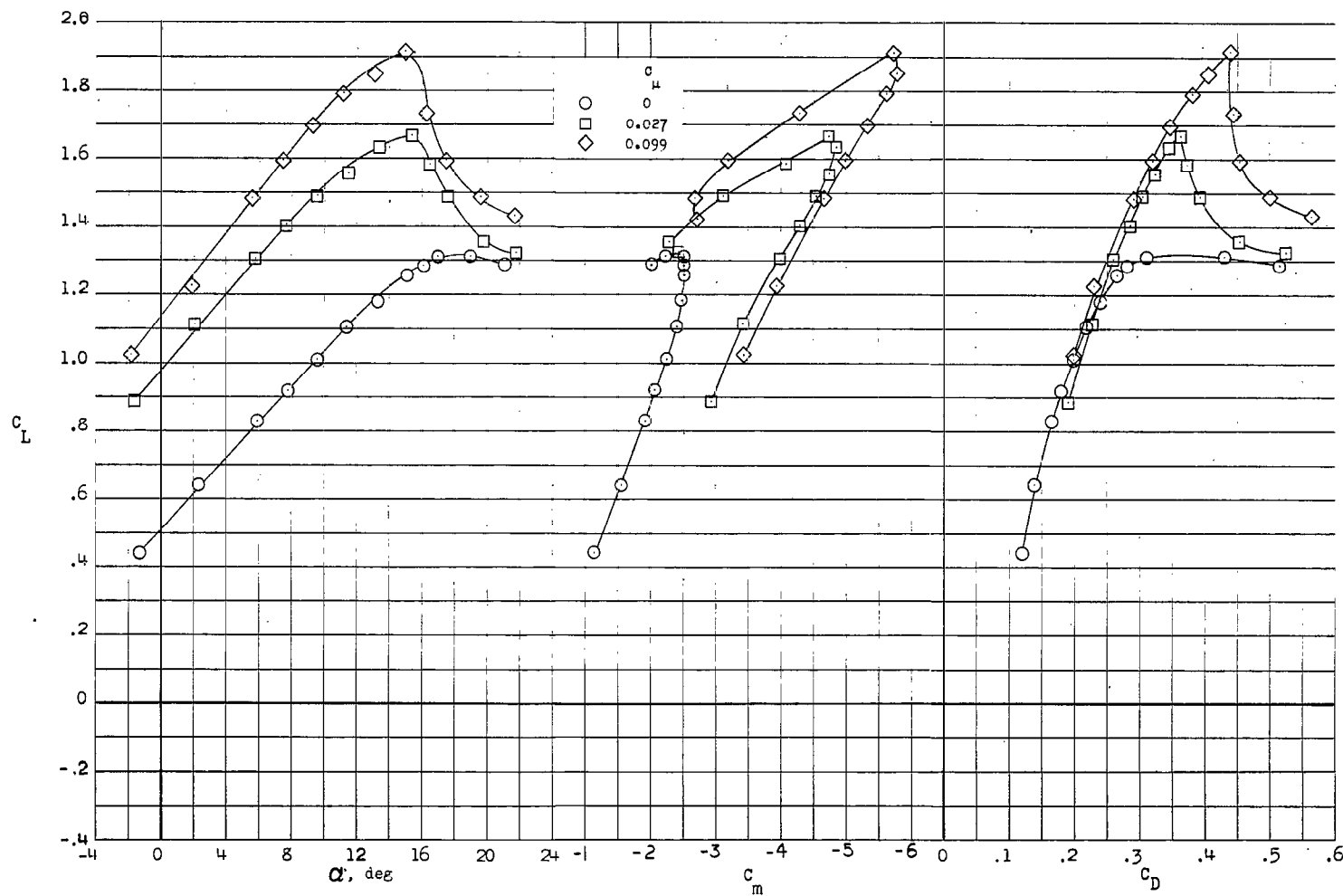
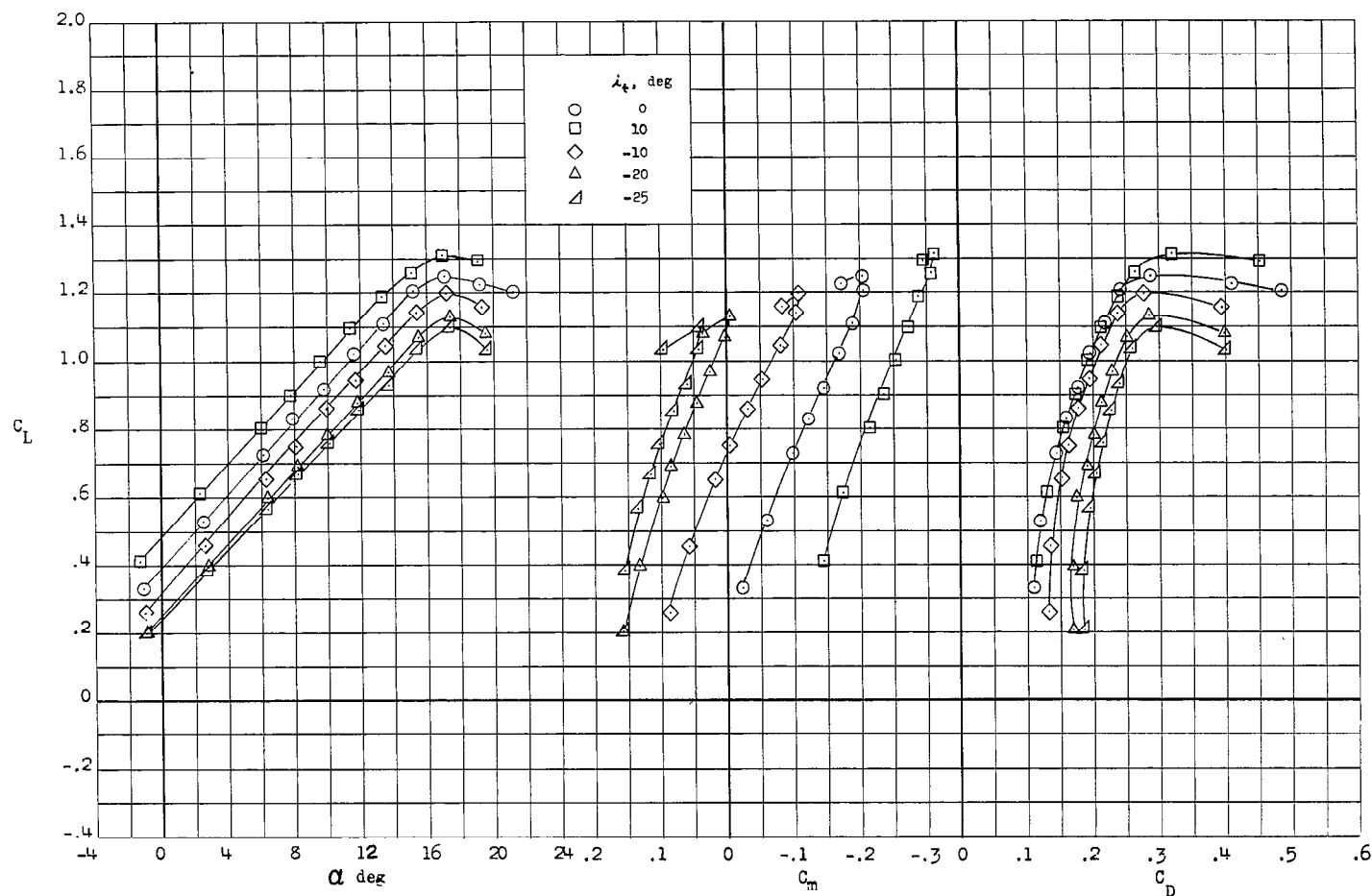
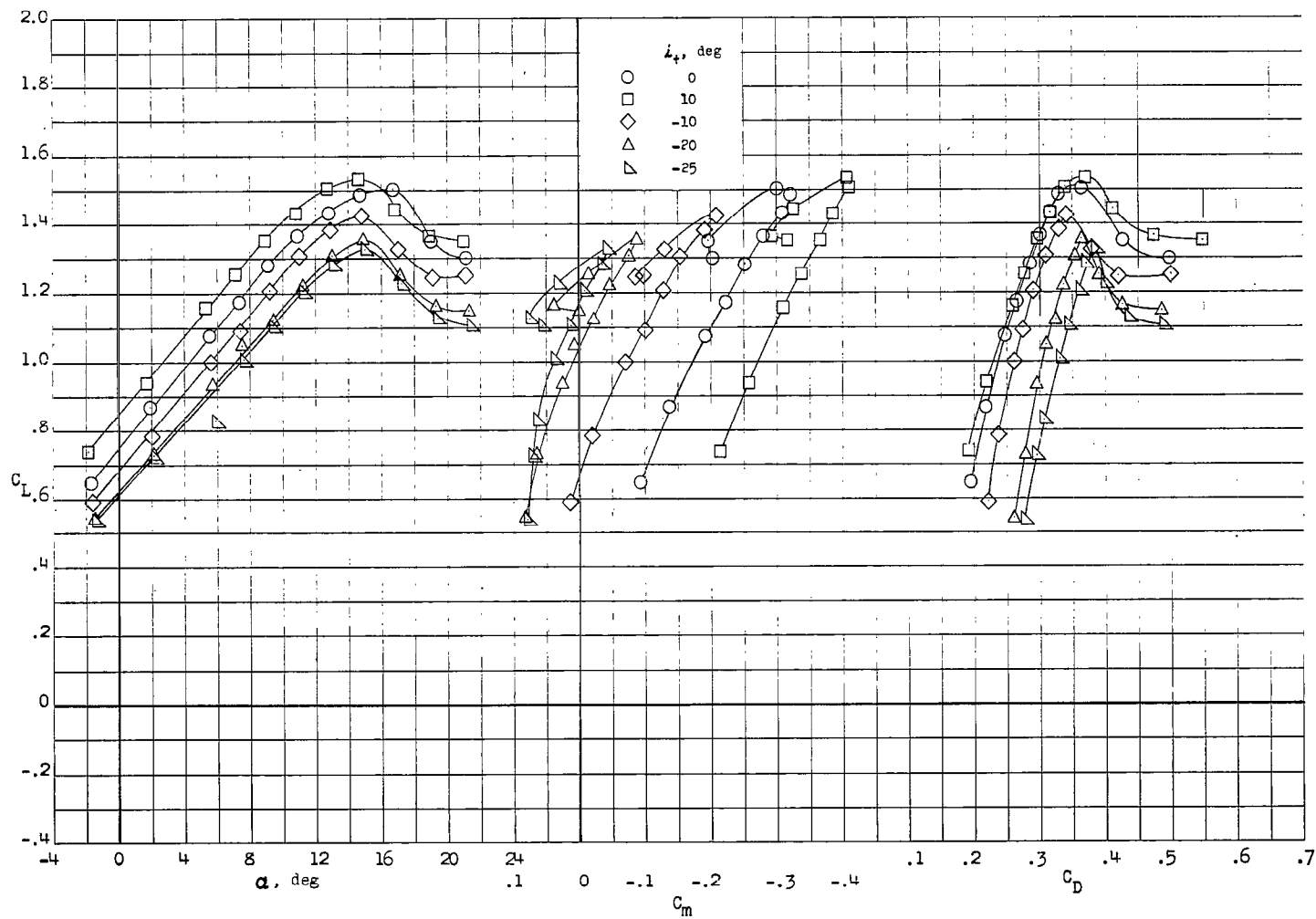


Figure 18.- Effect on the aerodynamic characteristics of drooping the aileron  $30^\circ$  with and without full-span trailing-edge blowing.  $0.60b/2$  slat plus radius increase installed;  $\delta_f = 60^\circ$ ;  $i_t = 0^\circ$ .



(a)  $C_{\mu} = 0.$

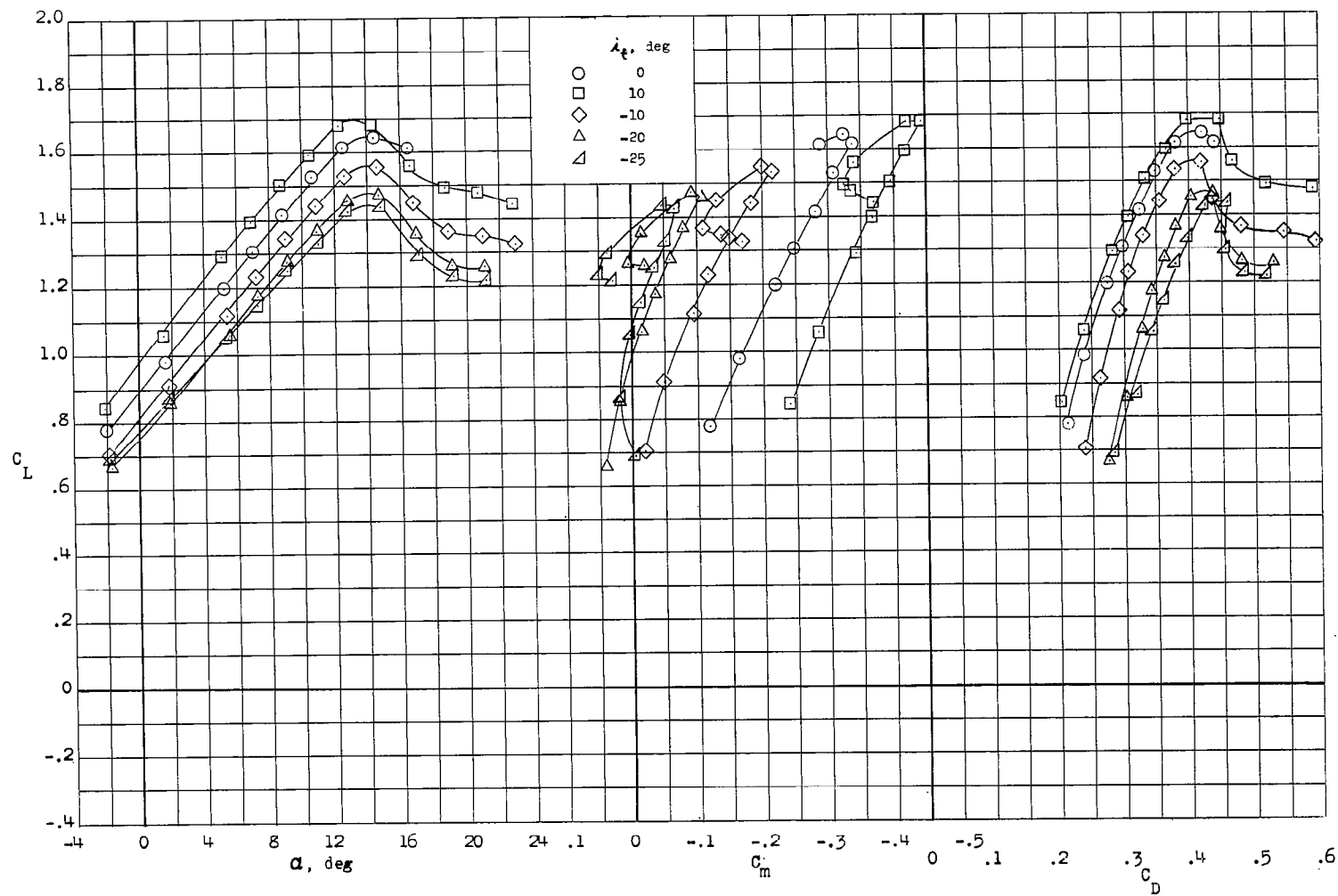
Figure 19.- Effect of horizontal-tail deflection on the aerodynamic characteristics with and without half-span trailing-edge blowing. 0.60b/2 slat plus radius increase installed.  $\delta_f = 60^\circ$ ;  $\delta_a = 0^\circ$ .



(b)  $C_{\mu} = 0.027$ .

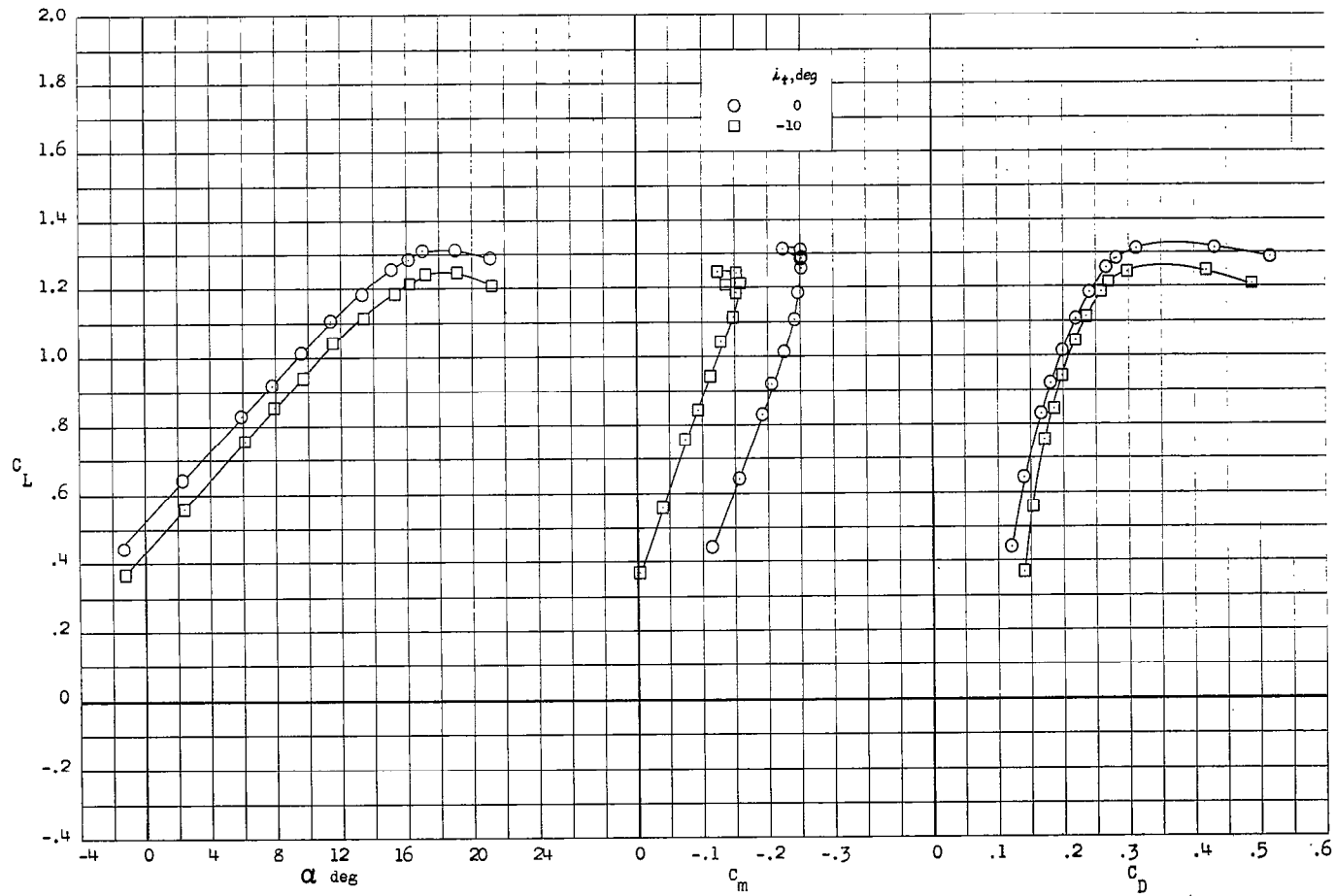
Figure 19.- Continued.





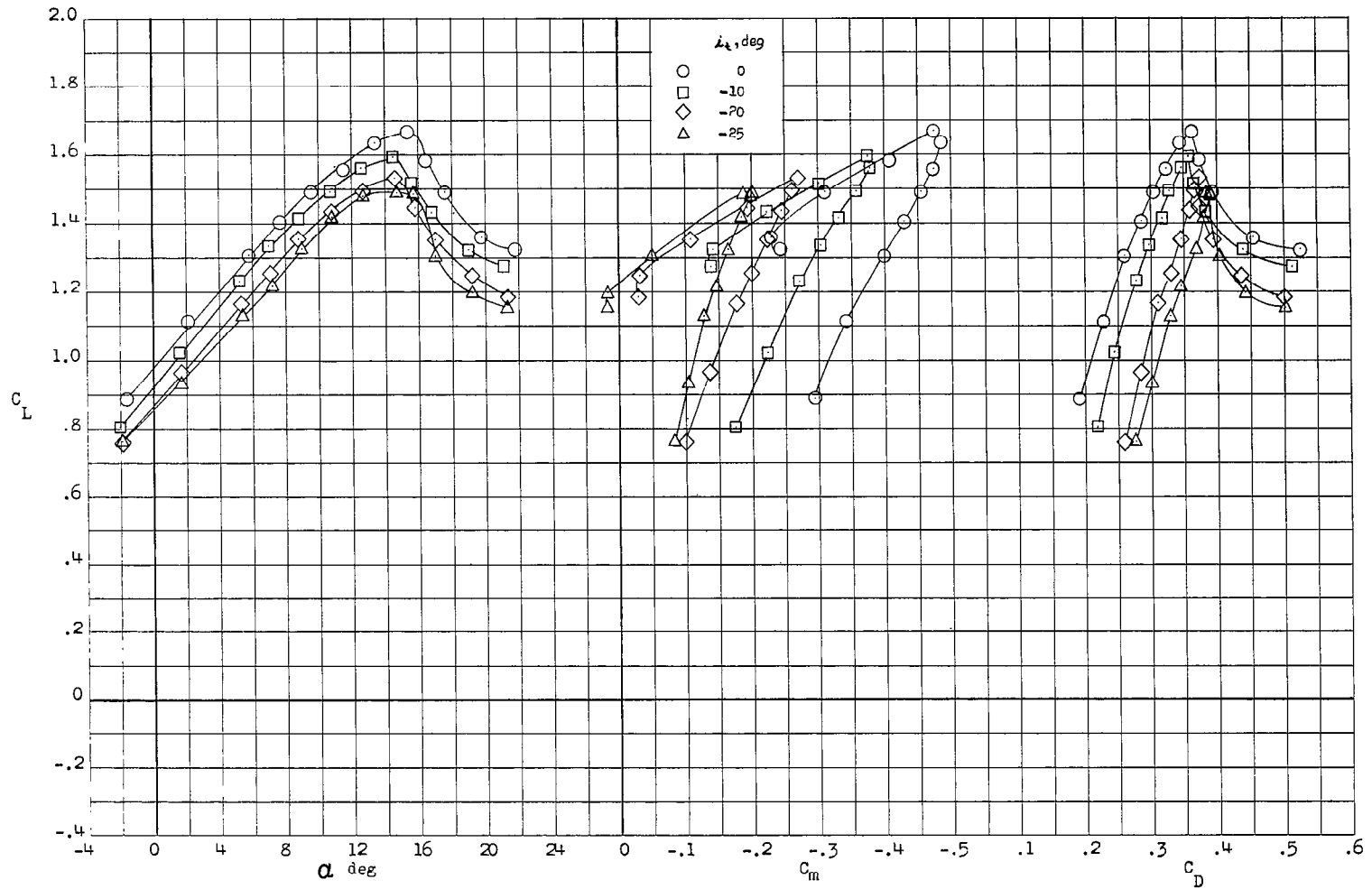
(c)  $C_{\mu} = 0.099$ .

Figure 19.- Concluded.



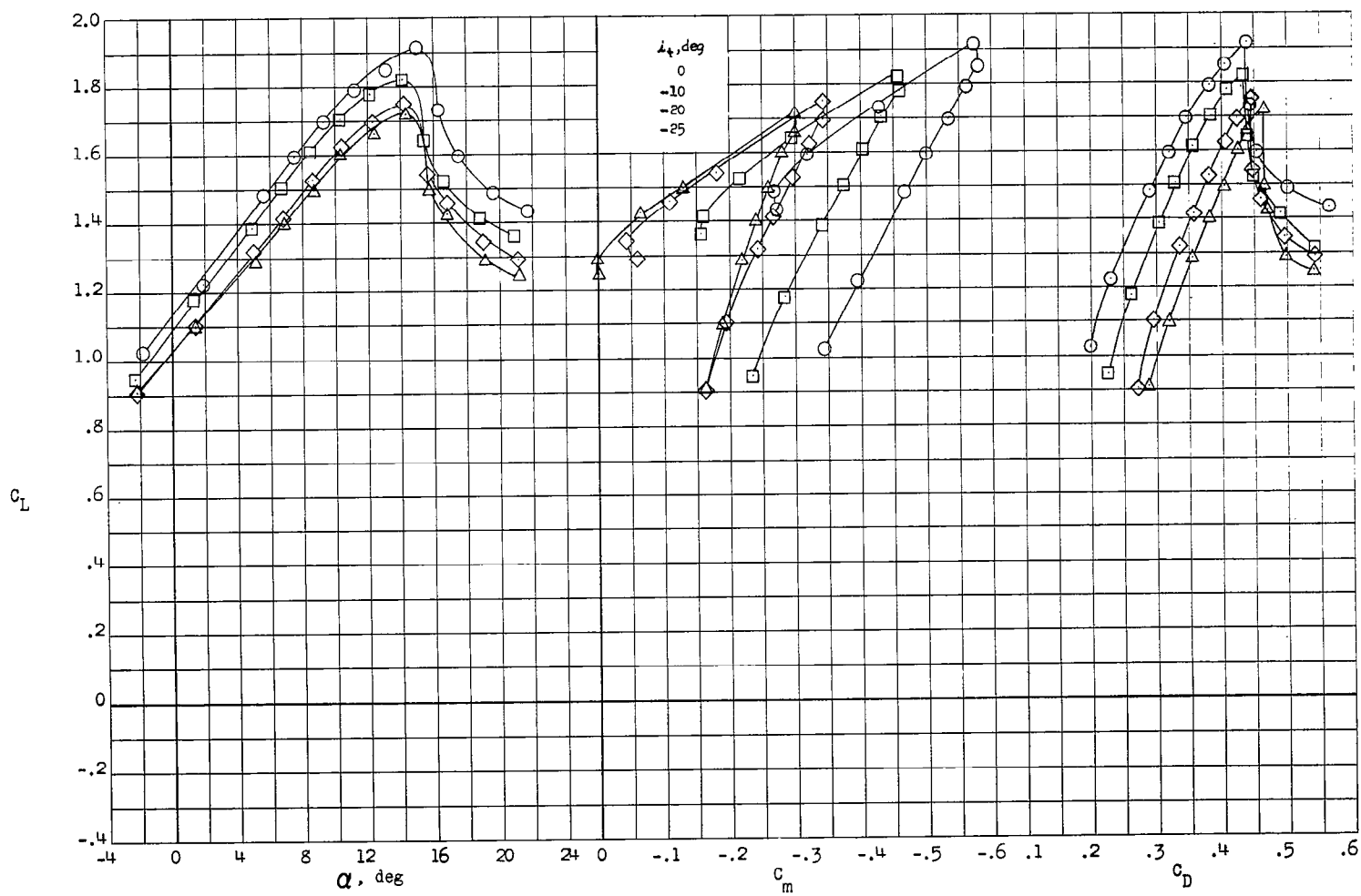
(a)  $C_{\mu} = 0$ .

Figure 20.- Effect of horizontal-tail deflection on the aerodynamic characteristics with and without full-span blowing over half-span flaps deflected  $60^\circ$  and  $30^\circ$  drooped ailerons.  $0.60b/2$  slat plus radius increase installed.



(b)  $C_{\mu} = 0.027$ .

Figure 20.- Continued.



(c)  $C_{\mu} = 0.099$ .

Figure 20.- Concluded.

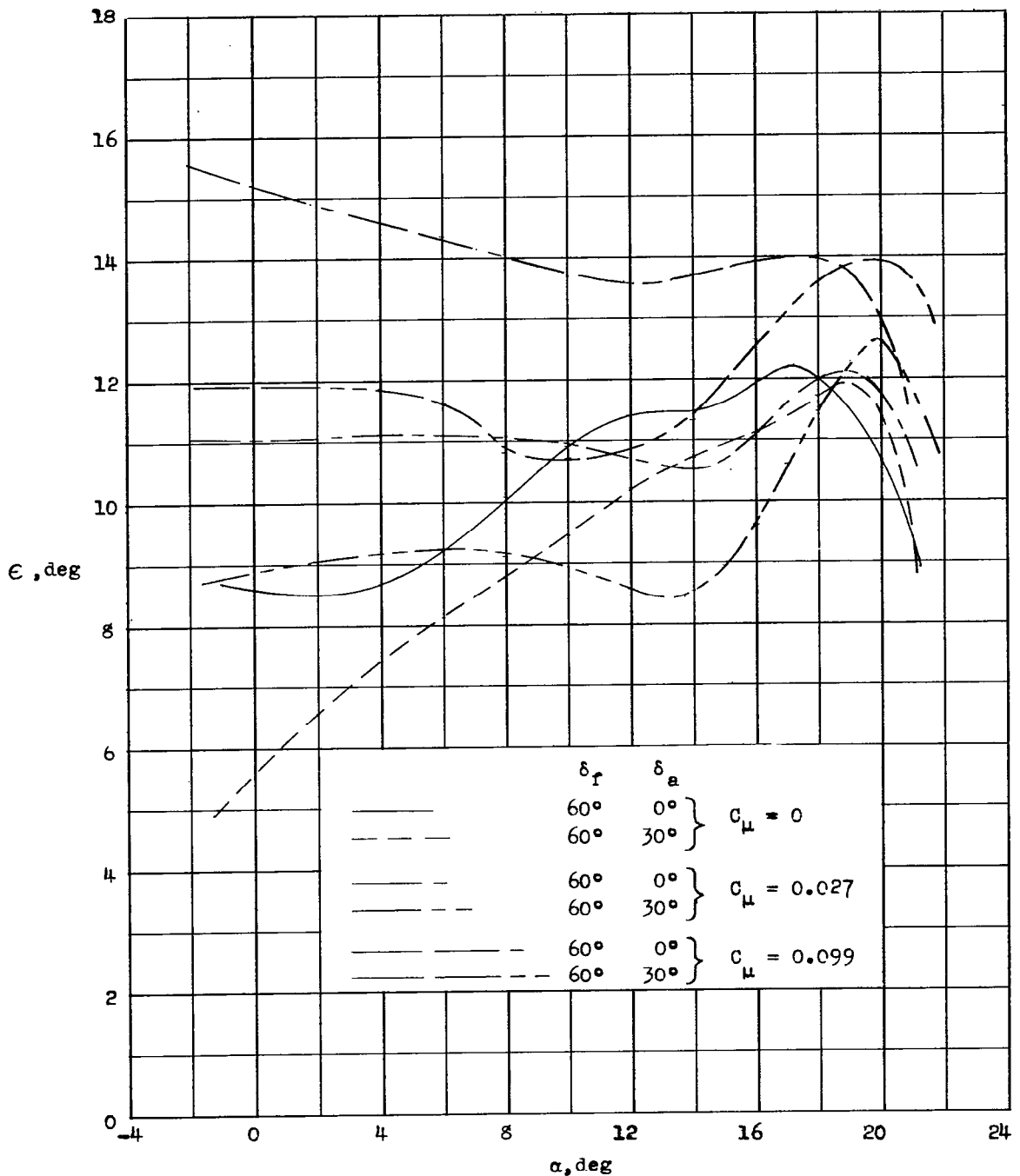
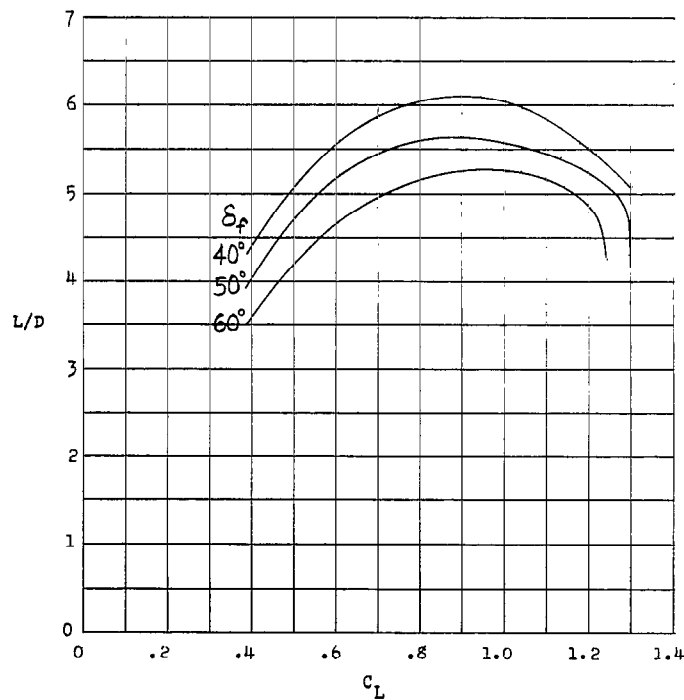
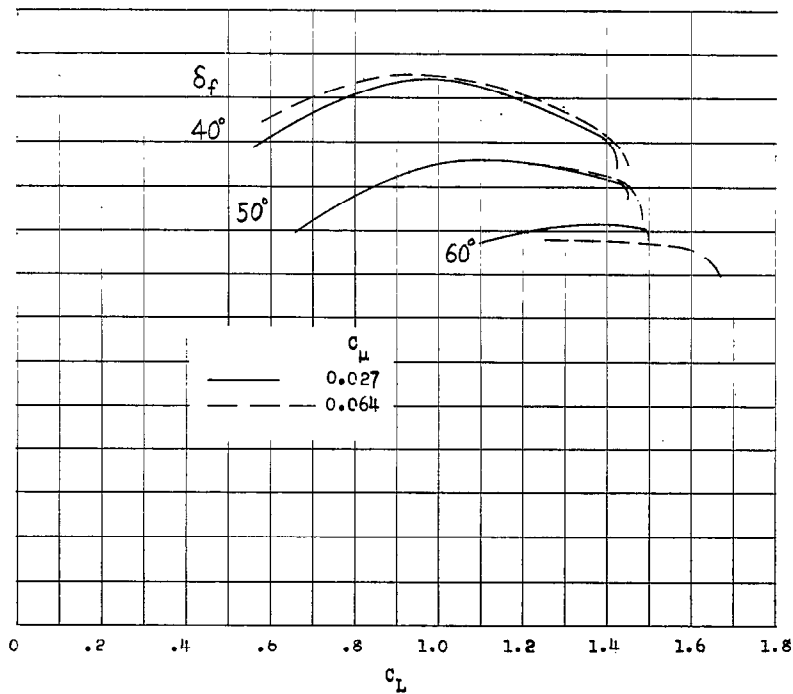


Figure 21.- Effect of trailing-edge blowing on the variation of effective downwash at the horizontal tail with angle of attack. 0.60b/2 slat plus radius increase installed.

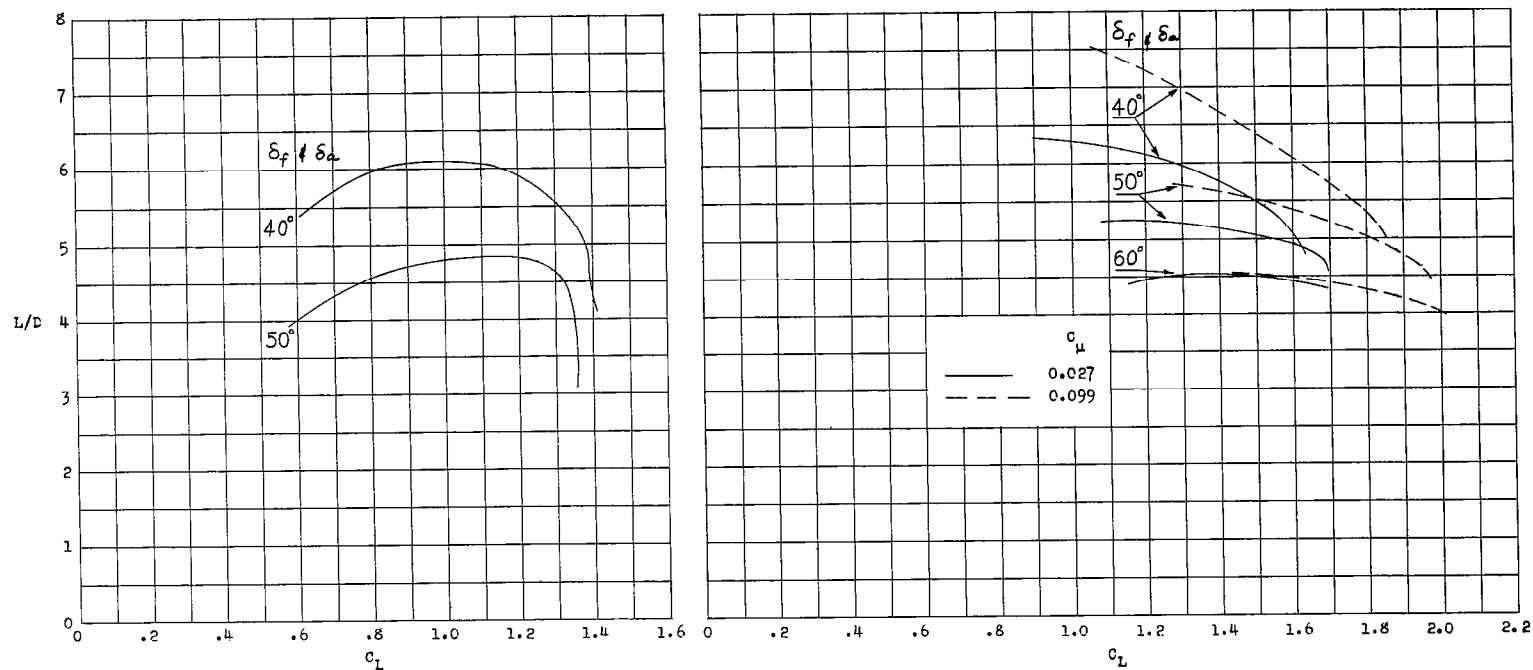


(a) Without trailing-edge blowing.



(b) With trailing-edge blowing.

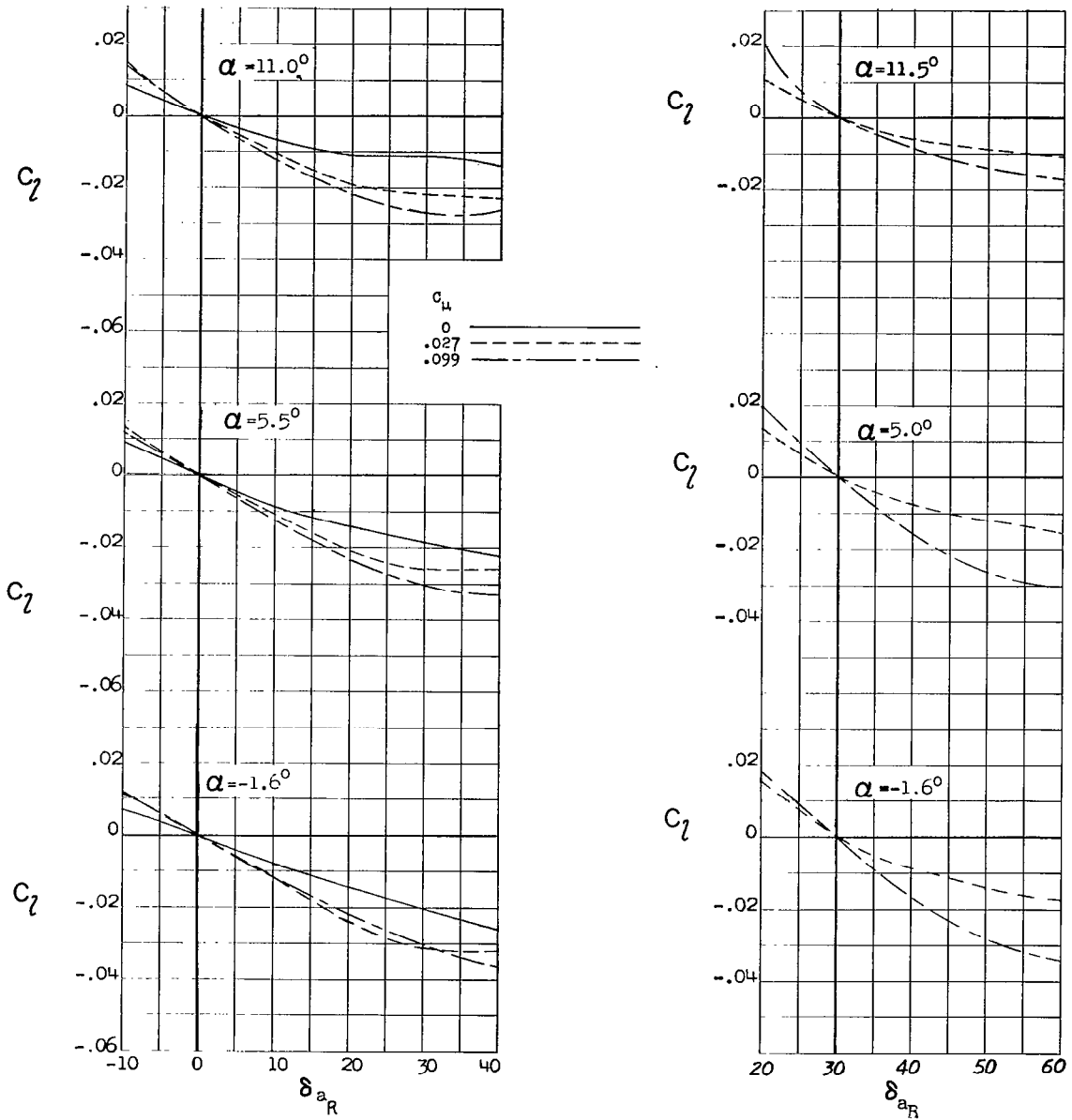
Figure 22.- Variation of lift-drag ratio  $L/D$  with  $C_L$  with and without trailing-edge blowing over half-span flaps.  $0.60b/2$  slat plus radius increase installed;  $\delta_a = 0^\circ$ ;  $i_t = 0^\circ$ .



(a) Without trailing-edge blowing.

(b) With trailing-edge blowing.

Figure 23.- Variation of lift-drag ratio  $L/D$  with  $C_L$  with and without trailing-edge blowing over full-span flaps. 0.60b/2 slat plus radius increase installed;  $i_t = 0^\circ$ .



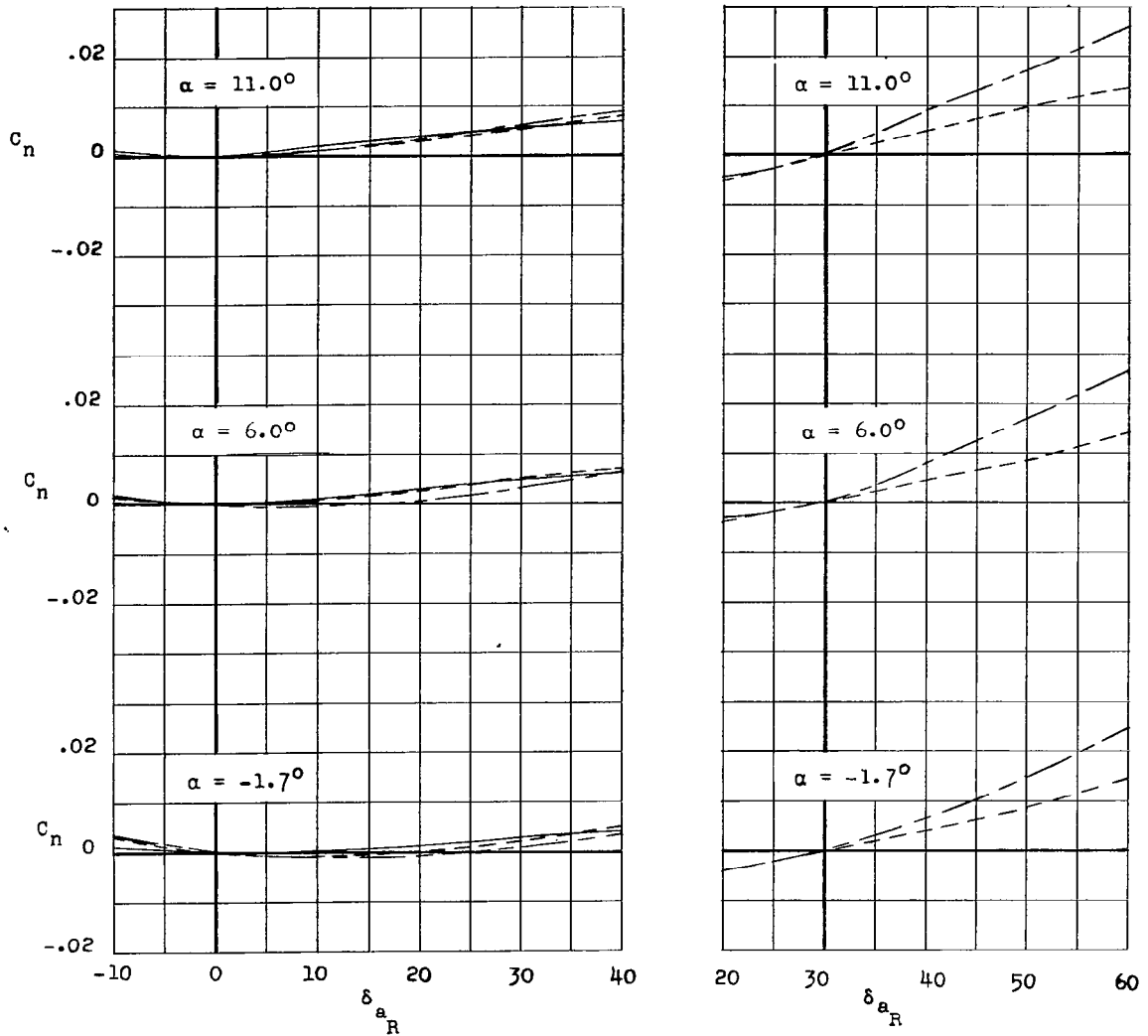
(a) Normal (undrooped) aileron;  
half-span trailing-edge  
blowing.

(b) 30° drooped aileron; full-  
span trailing-edge blowing.

Figure 24.- Effect of trailing-edge blowing on the aileron characteristics of a normal aileron and an aileron initially drooped 30°. 0.60b/2 slat plus radius increase installed;  $\delta_F = 60^\circ$ .

~~CONFIDENTIAL~~





(c) Normal (undrooped) aileron;  
half-span trailing-edge  
blowing.

(d)  $30^\circ$  drooped aileron; full-  
span trailing-edge blowing.

Figure 24.- Concluded.

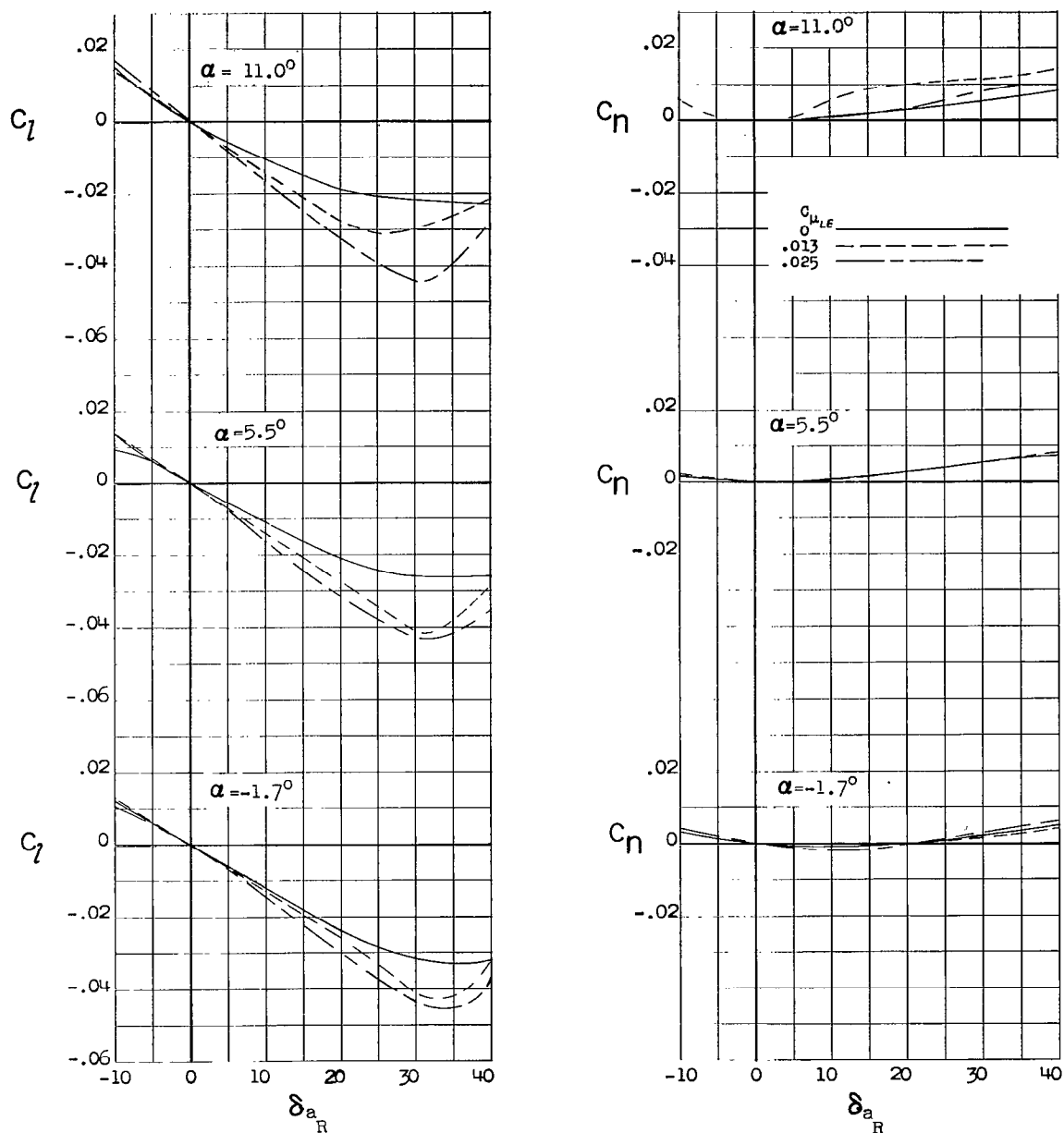


Figure 25.-- Effect of leading-edge blowing on the aileron characteristics of the model with blowing over half-span flaps.  $\delta_F = 60^\circ$ ;  $C_{\mu_{TE}} = 0.027$ ; full-span leading-edge radius increase installed.